Reviewer #1,

Comment: This manuscript by Yuan et al. reports a new algorithm to quantifying the heterogeneity in aerosol hygroscopicity, by using the data from H-TDMA. Average per-particle species diversity Dα, the bulk population species diversity Dγ, and their affine ratio χ was calculated as three indices to describe aerosol heterogeneity. These data are valuable and the figures presented in the paper are good description of the research. Therefore, I would suggest publication after the following comments have been addressed.

Reply**:** Thanks for the comments and suggestions. The point-by-point responses are listed below.

Comment: Specific comments:

(1) Line 28-29: "Considering that ambient aerosol particles in an aerosol population differ dramatically in chemical composition due to the complex sources and aging processes." The authors might find the following paper relevant findings from individual particle analysis by electron microscope and models. For example, recent studies focused on different kinds of mixing states such as Journal of Geophysical Research: Atmospheres 2022, 127, (5), e2021JD036055; Atmos. Chem. Phys.2021, 21, (23), 17727-17741; Environmental Science & Technology2021, 55, (24), 16339-16346.

Reply**:** Thanks for the comment. We have added these references. These literatures are crucial for perfecting this paper. They help to deepening and highlighting the significance of this study. (Lines 29-30, Page 2 in the revised manuscript)

(2) Line 43: may change from "black carbon (BC)-containing" to "black carbon-containing (BC-containing)"

Reply**:** Thanks for the comment. We have changed "black carbon (BC)-containing" to "black carbon-containing (BC-containing)". (Lines 43-44, Page 2 in the revised manuscript)

(3) Line 48: "most literature is" should use plural form

Reply**:** Thanks for the comment. We have replaced "most literature is" with "most studies are". (Line 48, Page 2 in the revised manuscript)

(4) Line 50: “we propose” -> “we proposed”

***Reply*:** Thanks for the comment. We have replaced “We propose” with “We proposed”. (Line 50, Page 2 in the revised manuscript)

(5) Line 59: “propose” should be “proposed”

***Reply*:** Thanks for the comment. This comment seems to be the same as comment 4. We have revised this sentence. (Line 50, Page 2 in the revised manuscript)

(6) Line 52: “will describe” should be described

***Reply*:** Thanks for the comment. We have replaced “will describe” with “described”. (Line 52, Page 2 in the revised manuscript)

(7) Line 53: “will be” should be “was”

***Reply*:** Thanks for the comment. We have replaced “will be” with “was”. (Line 53, Page 2 in the revised manuscript)

(8) Line 54: “are discussed” should be “were discussed”

***Reply*:** Thanks for the comment. We have replaced “are discussed” with “were discussed”. (Line 54, Page 2 in the revised manuscript)

(9) Line 55: “comes” should be “came”

***Reply*:** Thanks for the comment. We have changed “comes” to “came”. (Line 54, Page 2 in the revised manuscript)

(10) Line 81: why the font of “$TDMA_{fit}$” is different?

***Reply*:** Sorry for the mistake caused by the text editor. This is revised and the other font issues are also revised. (Line 81, Page 3 in the revised manuscript)

(11) Line 139: “ageing” is different with other “aging” in your article, here should be unified

***Reply*:** Thanks for the comment. We have changed “ageing” to “aging” in this line and we revised the whole text.

(12) Line 154: “ranges 1 to 2” should be added “from”

***Reply*:** Thanks for the comment. This sentence has been revised. (Line 160, Page 7 in the revised manuscript)

(13) Line 155-156: “it is 1 when … while 2 when …”, the grammar here is strange. May add “the” or “be” behind “while”

***Reply*:** Thanks for the comment. This sentence has been revised. (Line 162, Page 7 in the revised manuscript)

(14) Figure 2: Does blue represent the LH or grey represent the LH? Need explanations here.

***Reply*:** Thanks for the comment. The blue ball in Figure 2 represents the MH component and the grey ball represents the LH component. We have added the legend in Figure 2 to clearly show the LH and MH components. (Figure 2 in the revised manuscript)

(15) Line 186: why chose 110 nm aerosol? Need reasons here.

***Reply*:** Thanks for the comment. Here we want to focus primarily on the variation of the heterogeneity in aerosol hygroscopicity in the real atmosphere, especially for the condition that the total hygroscopicity of aerosol remained constant, to highlight the importance of the heterogeneity as an indicator for the evolution of aerosols.

From the time series of the heterogeneity for aerosols of the five measured sizes (40 nm, 80 nm, 110 nm, 150 nm, and 200 nm) during the selected episodes (Figure R1), we find the similar variation trends for aerosols larger than 100 nm. Difference is showed for the aerosol of 40 nm and 80 nm mainly due to their different formation mechanism, which will be further investigated in our following studies.

110 nm aerosol is chosen here by considering that 1) aerosol around 100 nm generally has the largest number concentration. Among the five measured sizes, the diameter of 110 nm aerosol is the closest to 100 nm. The heterogeneity in aerosol hygroscopicity of this diameter may have great

impact on the direct radiative forcing, especially for the condition with high relative humidity. 2) aerosol smaller than 100 mainly shows the gas to particle process in the atmosphere, while aerosol larger than 100 mainly reflects atmospheric aging process. The 110 nm aerosol lies in the transition zone between these two processes, the variation of the heterogeneity in 110 nm aerosol can better reflect the evolution of aerosol particles in the real atmosphere. Thus, we choose 110 nm aerosol as the example to show the variation characteristic.

We have added the reason in the revised manuscript. (Lines 187-195, Page 8 in the revised manuscript)

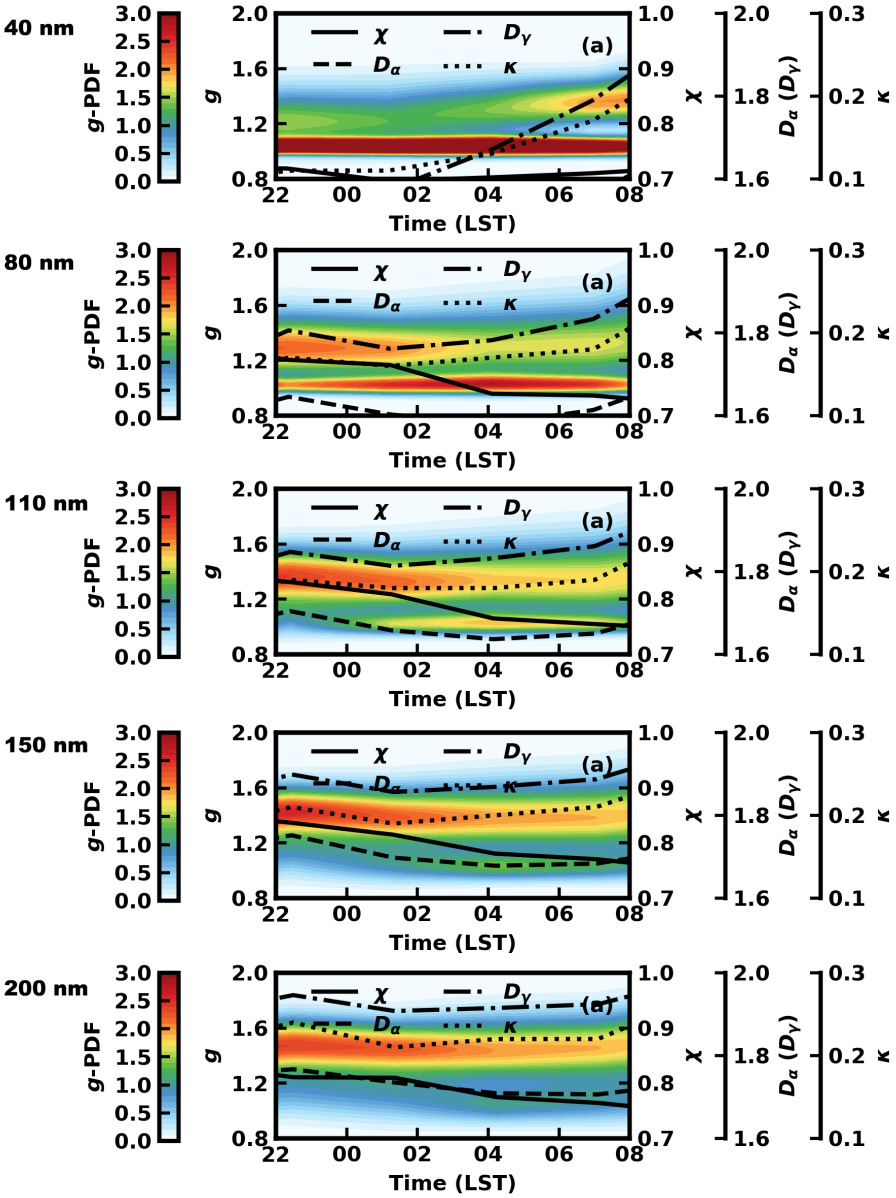

Figure R1. The variation of κ-PDF, D_α, D_γ, and χ during two typical evolution processes for aerosols of five measured diameters in the winter observation period.

(16) Line 190: why is χ high at night? Here needs more explanations.

***Reply*:** Thanks for the comment. Here we wanted to focus on the variation of the heterogeneity in aerosol hygroscopicity in the real atmosphere, especially for the condition that the total hygroscopicity of aerosol remained constant. Thus, just two episodes with tiny changes of κ_{mean} during the observation periods are chosen. These two episodes were both from the night to the morning on the next day and both χ showed high values at night with decreasing trend from the night to the morning.

To clearly explain this phenomenon, the diurnal variation of χ and aerosol particle number size distribution (PNSD) during the winter observation period is shown in Figure R2a. It can be found that χ had a relatively lower value than that in the afternoon at the traffic rush hour around 17:00-20:00 LST, which made the heterogeneous distribution of the LH and MH components within and between aerosol particles. Then χ gradually increased after the rush hour and had a relative higher value at night due to intensive mixing in the various atmospheric aging processes with less emissions, which led to the homogenous distribution of the LH and MH components in aerosols. This process was confirmed by the PNSD (Figure R1b) that the total number concentration decreased while the median diameter increased after the rush hour. The details in the variation characteristics will be further discussed in our following studies.

We revised Lines 196-200 to make the expression clearer. (Lines 196-200, Page 8 in the revised manuscript)

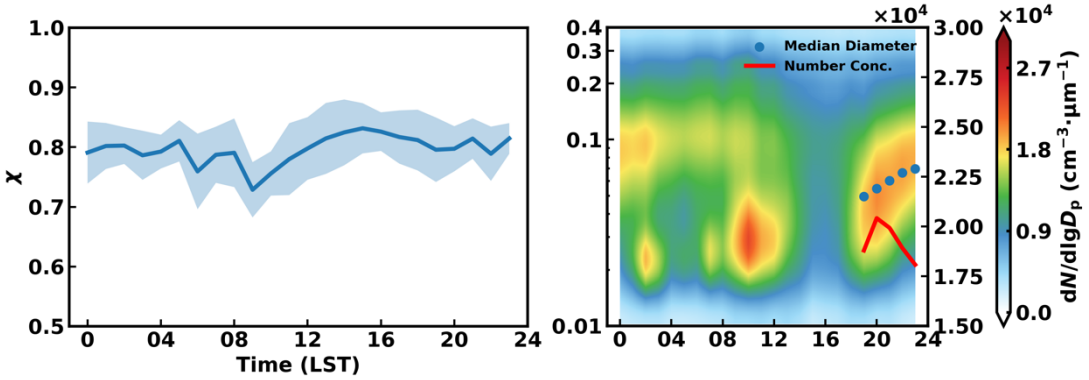

Figure R2. Diurnal variation of χ and PNSD during the winter observation period.

(17) Line 217: remove “will”

***Reply*:** Thanks for the comment. We have changed “will discuss” to “discussed”. (Line 230, Page 9 in the revised manuscript)

(18) Figure 6 (a) and (d) need a legend

***Reply*:** Thanks for the comment. The solid lines (blue) in (a) and (d) are the measured PNSD that can be fitted by a four-mode (a nucleation mode (NM), an Aitken mode (AM), an accumulation mode (AcM) and a coarse mode (CM)) lognormal distribution, which are represented by the thin solid line (orange), the dashed line (green), the dotted line (red), and the dash-dotted line (purple), respectively. We have added the legend in Figure 6 to clearly show the PNSD. (Figure 6 in the revised manuscript)

(19) Line 230: “Aitken mode” Why capitalize here?

***Reply*:** Thanks for the comment. “Aitken mode” is named after John Aitken, who is one of the founders of cloud physics and aerosol science. Thus, we capitalize “Aitken”.

Reviewer #2,

***Comment*:** This paper presents a method of how to derive metrics of diversity of a particle population with respect to hygroscopicity using H-TDMA measurements. The authors also demonstrate the use of their method by applying it to a dataset from the ambient atmosphere. This work fulfills an important need in our community, and I commend the authors on their contribution. So far, it has been very challenging to quantitatively derive these metrics from measurements since they rely on the quantitative knowledge of per-particle composition which have been challenging to obtain. Given that H-TDMA datasets have been collected in many different environments and could all be analyzed using the method described in this paper, this work has a great potential for deepening our understanding of aerosol mixing state in the ambient atmosphere and for providing much needed data to validate mixing-state-aware models.

The paper is concise and well-structured. It fits within the scope of ACP and I recommend publication after a few minor comments are taken into account.

***Reply*:** Thanks for the comments and suggestions. The point-by-point responses are listed below.

***Comment*:** Specific comments:

(1) line 21: The statement that heterogeneity in hygroscopicity is not considered in models is a little strong. Sectional models do capture the dependence in (average) hygroscopicity with size and modal model capture the variation in hygroscopicity for different sub-population. I suggest saying "not fully considered" or "not adequately considered". In fact, it is the case that many modeling approaches do provide some information about how hygroscopic and non-hygroscopic species are mixed (e.g., MAM4 in CESM) but so far, suitable measurement data has been lacking to validate these predictions. Developing a method to provide this kind of data is the contribution of this study.

***Reply*:** Thanks for the comment. We have revised the expression. (Lines 21-22, Page 1 in the revised manuscript)

(2) Nitpicky terminology comment: The term "aerosol" already refers to a population, so there is no need to say "aerosol population".

***Reply*:** Thanks for the comment. We have revised the expression for the whole manuscript.

(3) Line 32: Where the kappa-pdf is introduced would be a good place to cite Su et al., 2010, Atmos. Chem. Phys., 10, 7489–7503, 2010, where a general concept and mathematical framework of particle hygroscopicity distribution for the analysis and modeling of aerosol hygroscopic growth and CCN activity is presented.

***Reply*:** Thanks for the comment. We have added this reference. These literatures are crucial for perfecting this paper. They help to deepening and highlighting the significance of this study. (Lines 28-33, Page 2 in the revised manuscript)

(4) Explanation starting at line 104: This applies for one particular particle size, I suggest making this clear at the start of this section.

***Reply*:** Thanks for the comment. We revised this sentence to make the expression clearer. (Line 104, Page 4 in the revised manuscript)

(5) Equations 2 and 4: add limits to the integral.

***Reply*:** Thanks for the comment. These equations have been revised. (Equations 2 and 4 in the manuscript)

(6) Equations 8 and 9: suggest to not use ii as the counter variable. Use k or \ell, for example.

***Reply*:** Thanks for the comment. We have revised the counter variable and used "*j*" instead. (Lines 113-116, Page 5 in the revised manuscript)

(7) Line 141: Can you explain a bit more why kappa for the coarse mode is assumed to be 0? Couldn't you have non-hygroscopic primary particles in the coarse mode that have aged and acquired some coating materials that make the more hygroscopic (or at least increase their kappa to > 0)?

***Reply*:** Thanks for the comment. In this study, κ for the coarse mode is assumed to be 0 by considering that the primary chemical composition in this mode is nearly hydrophobic without aging and coating. The same assumption is applied in Chen et al. (2012). κ for larger particles is hard to be observed by H-TDMA technique so far, due to the technical bottleneck. Shen et al. (2021)

extended the H-TDMA measurement of aerosol hygroscopic properties to 600 nm in the urban environment, but for aerosol larger than 1 μm, κ can only be derived from the chemical composition according to the method used by Liu et al. (2014) and Gysel et al. (2007). As the reviewer mentioned, studies showed that aerosols larger than 1 μm are actually hygroscopic (Hegg et al., 2006; Massling et al., 2009; Liu et al., 2014), with κ slightly greater than 0.1 (Liu et al., 2014), due to the coating in atmospheric aging processes.

However, considering that aerosol particles larger than 1 μm generally have short lifetime and low number concentration except for the dusty weather, the influence of these particles on radiative forcing and cloud is limited. Also, the assumption that κ for the coarse mode is 0 can only have limited impact on the result of the size-resolved heterogeneity. More importantly, this section focuses on the application of the proposed algorithm. If κ-PDF for aerosols larger than 1 μm could be obtained in the future, it could be directly applied in the framework provided by our study to discuss the size-resolved heterogeneity in aerosol hygroscopicity and its impact on aerosol climatical and environmental effects.

This discussion is added in the revised manuscript. (Lines 143-148, Page 6 in the revised manuscript)

(8) Line 170-173: These sentences are unclear, can you please rephrase?

***Reply*:** Thanks for the comment. We have revised this paragraph in the manuscript. (Lines 173-178, Pages 7-8 in the revised manuscript)

(9) In the introduction/conclusion, you could stress more explicitly that existing H-TDMA datasets could be analyzed using this algorithm. This could have a large impact on how we use and think about these datasets and will help providing data for constraining models.

***Reply*:** Thanks for the comment. This suggestion deepens the significance of our work, and we added this discussion in the results and conclusions section to further show the importance of this work. (Lines 184-185, Page 8 and Lines 283-287, Page 11 in the revised manuscript)

References

Chen, J., Zhao, C., Ma, N., Liu, P., Göbel, T., Hallbauer, E., Deng, Z., Ran, L., Xu, W., Liang, Z., et

al.: A parameterization of low visibilities for hazy days in the North China Plain, Atmospheric Chemistry and Physics, 12, 4935–4950, https://doi.org/10.5194/acp-12-4935-2012, 2012.

Gysel, M., Crosier, J., Topping, D., Whitehead, J., Bower, K., Cubison, M., Williams, P., Flynn, M., McFiggans, G., and Coe, H.: Closure study between chemical composition and hygroscopic growth of aerosol particles during TORCH2, Atmospheric Chemistry and Physics, 7, 6131–6144, https://doi.org/10.5194/acp-7-6131-2007, 2007.

Hegg, D., Covert, D. S., Crahan, K., Jonsson, H., and Liu, Y.: Measurements of aerosol size-resolved hygroscopicity at sub and supermicron sizes, Geophysical research letters, 33, L21808, https://doi.org/10.1029/2006GL026747, 2006.

Liu, H., Zhao, C., Nekat, B., Ma, N., Wiedensohler, A., Van Pinxteren, D., Spindler, G., Müller, K., and Herrmann, H.: Aerosol hygroscopicity derived from size-segregated chemical composition and its parameterization in the North China Plain, Atmospheric Chemistry and Physics, 14, 2525–2539, https://doi.org/10.5194/acp-14-2525-2014, 2014.

Massling, A., Stock, M., Wehner, B., Wu, Z., Hu, M., Brüggemann, E., Gnauk, T., Herrmann, H., and Wiedensohler, A.: Size segregated water uptake of the urban submicrometer aerosol in Beijing, Atmospheric Environment, 43, 1578–1589, https://doi.org/10.1016/j.atmosenv.2008.06.003, 2009.

Shen, C., Zhao, G., Zhao, W., Tian, P., and Zhao, C.: Measurement report: aerosol hygroscopic properties extended to 600 nm in the urban environment, Atmospheric Chemistry and Physics, 21, 1375–1388, https://doi.org/10.5194/acp-21-1375-2021, 2021.

Quantifying particle-to-particle heterogeneity in aerosol hygroscopicity

Liang Yuan[1, 2] and Chunsheng Zhao[2, *]

[1]Chengdu Plain Urban Meteorology and Environment Scientific Observation and Research Station of Sichuan Province, School of Atmospheric Sciences, Chengdu University of Information Technology, Chengdu 610225, China
[2]Department of Atmospheric and Oceanic Sciences, School of Physics, Peking University, Beijing, 100871, China

Correspondence: Chunsheng Zhao (zcs@pku.edu.cn)

Abstract. The particle-to-particle heterogeneity in aerosol hygroscopicity is crucial for understanding aerosol climatic and environmental effects. The hygroscopic parameter κ, widely applied to describe aerosol hygroscopicity for ~~aerosol populations~~ aerosols both in models and observations, is a probability distribution highly related to aerosol heterogeneity due to the complex sources and aging processes. However, the heterogeneity in aerosol hygroscopicity is not adequately represented in observations and model simulations, leading to challenges in accurately estimating aerosol climatic and environmental effects. Here, we propose an algorithm for quantifying the particle-to-particle heterogeneity in aerosol hygroscopicity, based on information-theoretic entropy measures, by using the data that comes only from the in-situ measurement of the hygroscopicity tandem differential mobility analyzer (H-TDMA). ~~Aerosol populations~~ Aerosols in this algorithm are assumed to be simple binary systems consisting of the less hygroscopic and more hygroscopic components, which are commonly used in H-TDMA measurement. Three indices, including the average per-particle species diversity D_α, the bulk population species diversity D_γ, and their affine ratio χ, are calculated from the probability distribution of κ to describe aerosol heterogeneity. This algorithm can efficiently characterize the evolution of aerosol heterogeneity with time in the real atmosphere. Our results show that the heterogeneity varies much with aerosol particle size and large discrepancies exist in the width and peak value of particle number size distribution (PNSD) with varied heterogeneity after hygroscopic growth, especially for conditions with high relative humidity. This reveals a vital role of the heterogeneity in ambient PNSD and significant uncertainties in calculating the climate-relevant properties if the population-averaged hygroscopicity is applied by neglecting its heterogeneity. This work points the way toward a better understanding of the role of hygroscopicity in evaluating aerosol climatic and environmental impacts.

1 Introduction

Aerosol hygroscopicity describes the interaction of ~~aerosols~~ aerosol particles and water vapor and severely influences aerosol climatic and environmental effects (Wang and Chen, 2019; Swietlicki et al., 2008; Liu et al., 2013; Tie et al., 2017). It is highly related to the particle-to-particle heterogeneity in aerosol hygroscopicity, which is crucial but ~~not~~ not adequately considered in observations and models, posing a challenge in accurately estimating aerosol effects on climate and environment.

Köhler theory (Köhler, 1936) is the basis of the studies on aerosol hygroscopicity. Nowadays, the most widely used parameter to describe aerosol hygroscopicity in observations and models is the hygroscopicity parameter, κ, proposed in κ-Köhler

theory (Petters and Kreidenweis, 2007). κ extends and facilitates the application of Köhler theory (Zieger et al., 2013; Bian et al., 2014; Chen et al., 2014; Tao et al., 2014; Brock et al., 2016) and can be expediently observed under both subsaturated (Liu et al., 1978; Kuang et al., 2017) and supersaturated conditions (Petters and Kreidenweis, 2007; Cai et al., 2018). It can also be derived from the observed chemical composition (Liu et al., 2014). Considering that ambient aerosol particles in an ~~aerosol population~~ aerosol differ dramatically in chemical composition due to the complex sources and aging processes ~~. In~~ (Li et al., 2021; Zheng et al., 2021; Pang et al., 2022), in terms of aerosol hygroscopicity, the distribution of the nearly hydrophobic (NH), the less hygroscopic (LH), and the more hygroscopic (MH) components (Liu et al., 2011; Tan et al., 2013b; Yuan et al., 2020) vary between and within particles~~. Such~~ , such particle-to-particle heterogeneity in aerosol hygroscopicity results in a probability distribution of κ (κ-PDF) for an aerosol ~~population.~~ (Su et al., 2010). Among the three above-mentioned observing techniques, although the hygroscopicity tandem differential mobility analyzer (H-TDMA) can directly achieve κ-PDF under subsaturated condition, which is essential to investigate the hygroscopicity and activation property of ~~aerosol populations~~aerosols, most studies focus on the analysis and application of the population-averaged κ (~~κ_{mean}~~ κ_{mean}) by neglecting the heterogeneity (Chen et al., 2014; Tao et al., 2014; Brock et al., 2016; Kuang et al., 2017; Liu et al., 1978; Cai et al., 2018; Liu et al., 2014; Yuan et al., 2020; Wang et al., 2018), leading to uncertainties in the estimation of aerosol impacts on climate and environment.

Many research fields face the problem of heterogeneity involving the diversity of variables or issues. The diversity ~~is~~ was first quantified in Whittaker (1972) by introducing the information-theoretic entropy in ecology and then in many other fields, including economics (Drucker, 2013), immunology (Tsimring et al., 1996), neuroscience (Strong et al., 1998), and genetics (Falush et al., 2007). Riemer and West (2013) applied it in atmospheric science for the research of aerosol mixing state. By referring to Whittaker (1972) and Riemer and West (2013), the impact of the mixing state of ~~black carbon (BC)-containing~~ black carbon-containing (BC-containing) particles on light absorption enhancement ~~is~~ was investigated, which ~~shows~~ showed that absorption is strongly affected by the heterogeneity of BC-containing ~~aerosol population and explains~~ aerosol and explained that the discrepancy between simulated and observed absorption enhancement accounts for the particle-to-particle heterogeneity in composition (Fierce et al., 2016, 2020; Zhao et al., 2021). How crucial the heterogeneity in aerosol hygroscopicity is for the highly climate-relevant aerosol size distribution, optical, and activation properties? However, to the best of the authors' knowledge, ~~most literature is~~ most studies are not focused on quantitatively evaluating the heterogeneity concerning aerosol hygroscopicity for in-situ measurements.

Given these considerations, ~~we propose~~ we proposed an algorithm for quantifying the particle-to-particle heterogeneity in aerosol hygroscopicity in the real atmosphere. This algorithm is based on information-theoretic entropy measures, employing observed data from the in-situ measurement of H-TDMA. In the following, section 2 ~~will describe the detail of the algorithm; The~~ described the algorithm in detail and the interpretation of the results from the algorithm ~~will be~~ was presented in section 3. The importance of the heterogeneity and the application of the algorithm ~~are~~ were discussed and also included in section ~~3;~~ 3. The last section ~~comes the conclusions~~came the conclusions.

2 Data and Methods

2.1 Measurement site

The campaign was implemented for two periods from 23 January to 25 February and 19 July to 8 September 2019, respectively, at the meteorological station (30.58°N, 103.98°E) inside the campus of Chengdu University of Information and Technology (CUIT) located in Shuangliu district, southwest of the main urban area of Chengdu, China. The elevation of the observation site is approximately 500 m. Fig. S1 in the supplemental file shows the map of the site. It is surrounded by residential neighbourhoods with no nearby sources of significant industrial pollution. Aerosol particles here are representative of the urban environments. More details can be found in Yuan et al. (2020)

2.2 Data of H-TDMA measurement

A custom-built H-TDMA designed by Tan et al. (2013a) ~~is~~ was employed to obtain the hygroscopic properties for ~~aerosols~~ aerosol particles with dry diameters $D_{\mathrm{p}}(\mathrm{Dry})$ of 40, 80, 110, 150, and 200 nm. The schematic structure of the H-TDMA is shown in Fig. S2 in the supplemental file. This H-TDMA ~~is~~ was placed in a temperature-controlled (25 °C) container, with an aerosol inlet equipped with a $PM_{2.5}$ impactor that ~~extends~~ extended out of the container from the roof and set approximately 3 m above ground. It mainly consists of two differential mobility analyzers (DMA) (Model 3081A, TSI Inc., USA), a humidification system and a condensation particle counter (CPC) (Model 3787, TSI Inc., USA). Aerosol samples with a flow of 0.6 $\mathrm{L}\cdot\mathrm{min}^{-1}$ are first introduced into a Nafion dryer (Model MD-700-24S-3, Perma Pure Inc., USA) by an external vacuum pump to maintain the RH below 10%. These ~~aerosols~~ aerosol particles flow through an advanced aerosol X-ray neutralizer (Model 3088, TSI Inc., USA) to be single-charged and are then screened by the first DMA ~~(DMA1)~~(DMA-1) with set voltages. Subsequently, the selected quasi-monodisperse dry ~~aerosols~~ particles feed into a Nafion humidifier (Model PD-07018T-24MSS, Perma Pure Inc., USA) with RH of 90% (±0.3%). Finally, the PNSDs of humidified particles out of the humidifier are measured by the second DMA ~~(DMA2)~~(DMA-2) coupled with the CPC. The details of the H-TDMA refer to Yuan et al. (2020).

The growth factor ~~(g)~~ of the quasi-monodisperse ~~aerosols $g[D_{\mathrm{p}}(\mathrm{Dry})]$ selected by the first differential mobility analyzer (DMA)~~ aerosol particles $g[D_{\mathrm{p}}(\mathrm{Dry})]$ selected by DMA-1 equipped in the H-TDMA can be then calculated by:

$$g[D_{\mathrm{p}}(\mathrm{Dry})] = \frac{D_{\mathrm{p}}(\mathrm{RH})}{D_{\mathrm{p}}(\mathrm{Dry})}, \tag{1}$$

where $D_{\mathrm{p}}(\mathrm{RH})$ represents the particle diameter screened by ~~DMA2~~ DMA-2 at a specific relative humidity (RH), e.g., 90% in this study. The measured distribution function of g (g-MDF) is calculated from aerosol particle number size distribution (PNSD) counted by the CPC installed downstream of ~~the second DMA. The $\mathrm{TDMA}_{\mathrm{fit}}$~~ DMA-2. The $\mathrm{TDMA}_{\mathrm{fit}}$ algorithm (Stolzenburg and McMurry, 2008) is employed to convert the g-MDF to the actual probability distribution function (g-PDF) in the campaign (Gysel et al., 2009). For each measured dry diameter, the g-PDFs are thereafter normalized as:

$$\int_{1}^{\infty} c(g)\mathrm{d}g = 1, \tag{2}$$

where, $c(g)$ represents the normalized g-PDF. For each g, κ can be converted using κ-Köhler theory (Petters and Kreidenweis, 2007):

$$\kappa = (g^3 - 1) \times \left[\frac{1}{RH} \times \exp\left(\frac{4\sigma_{s/a} M_{\mathrm{w}}}{RT\rho_{\mathrm{w}} D_{\mathrm{p}}(\mathrm{Dry}) g}\right) - 1\right], \tag{3}$$

where $\sigma_{\mathrm{s/a}}$ of 0.072 $\mathrm{J \cdot m^{-2}}$ is the surface tension of the solution/air interface~~;~~, M_{w} of 18.015 $\mathrm{g \cdot mol^{-1}}$ is the molecular weight of water~~;~~, ρ_{w} of 1.0 $\mathrm{g \cdot cm^{-3}}$ is the density of water~~;~~, R of 8.315 $\mathrm{J \cdot K^{-1} \cdot mol^{-1}}$ is the universal gas constant~~;~~, and T of 298.15 K is the temperature in Kelvin. Then, the κ-PDF can be obtained and normalized as:

$$\int_{0}^{\infty} c(\kappa)\mathrm{d}\kappa = 1, \tag{4}$$

where $c(\kappa)$ is the normalized κ-PDF as the examples shown in Fig. 1.

2.3 Calculation of the heterogeneity in aerosol hygroscopicity

The particle-to-particle heterogeneity in aerosol hygroscopicity is calculated by using the H-TDMA measured κ-PDF (e.g. the exmaples in Fig. 1). The key assumption is that an ~~aerosol population~~ aerosol containing N aerosol particles is a binary system consisting of the LH and MH components with respective κ of 0.01 (κ_{LH}) (typical for organics) and 0.6 (κ_{MH}) (typical for sulphate and nitrate). Each aerosol particle in the population contains one or two of the LH and MH components and thus their κ varied between 0.01 and 0.6. κ-PDF of the ~~aerosol population~~ aerosol can be considered as the normalized aerosol number fractions varied with κ between ~~0.1~~ 0.01 and 0.6 (Fig. 1). The volume fraction of these two components in each aerosol particle can be calculated based on κ according to the ZSR rule (Zdanovskii, 1948; Stokes and Robinson, 1966).

By refering to information-theoretic entropy measures (Whittaker, 1972; Riemer and West, 2013; Zhao et al., 2021), three indices, including the average per-particle species diversity D_α, the bulk population species diversity D_γ, and their affine ratio χ, are calculated to together describe the heterogeneity. The details are described as follows:

Firstly, for the ~~aerosol population with a~~ aerosol with a given dry diameter and a known κ-PDF with X bins, the volume fraction of the LH and MH components at bin i (i=1, 2, 3, …, X), $P_{i,\mathrm{LH}}$ and $P_{i,\mathrm{MH}}$, can be calculated by the combination of ~~Eqs. 5 and 6.~~

$$P_{i,\mathrm{LH}} + P_{i,\mathrm{MH}} = 1, \tag{5}$$

and

$$P_{i,\mathrm{LH}} \times \kappa_{\mathrm{LH}} + P_{i,\mathrm{MH}} \times \kappa_{\mathrm{MH}} = \kappa_i, \quad (6)$$

where κ_i is the κ at bin i.

Secondly, the mixing entropy for particles at bin i (H_i) can be calculated by

$$H_i = -P_{i,\mathrm{LH}} \times \ln P_{i,\mathrm{LH}} - P_{i,\mathrm{MH}} \times \ln P_{i,\mathrm{MH}}. \quad (7)$$

Then the average particle mixing entropy for the ~~aerosol population~~ aerosol (H_α) is calculated by

$$H_\alpha = \sum_{ii=1}^{N} P_{ii} \times H_{ii}, \quad (8)$$

where, ~~H_{ii}~~ H_i is the mixing entropy for particle ~~ii~~ (ii) i (i=1, 2, 3, ..., N) ~~; P_{ii}~~ in the aerosol. P_i is the volume proportion of particle ~~ii~~ i to the total volume of the ~~aerosol population~~aerosol, which is calculated by

$$P_{ii} = \frac{V_{ii}}{V_{\mathrm{total}}} \frac{V_i}{V_{\mathrm{total}}} = \frac{1}{N}, \quad (9)$$

because all particles have the same diameters. Considering that particles in the same κ bin have the same physical and chemical properties, they have the same mixing entropy. Eqs. 8 and 9 can be simplified as

$$H_\alpha = \sum_{i=1}^{X} \frac{1}{N} \times H_i \times c(\kappa)_i \times \Delta\kappa, \quad (10)$$

where, $c(\kappa)_i$ is the probability density value of the normalized κ-PDF at bin i, and $\Delta\kappa$ is the bin width.

Additionally, the population-level mixing entropy (H_γ) is calculated by

$$H_\gamma = -P_{\mathrm{LH}} \times \ln P_{\mathrm{LH}} - P_{\mathrm{MH}} \times \ln P_{\mathrm{MH}}, \quad (11)$$

where, P_{LH} and P_{MH} are the respective volume fraction of the LH and MH components in the population and calculated by

$$P_{\mathrm{LH}} = \sum_{i=1}^{X} P_{i,\mathrm{LH}} \times c(\kappa)_i \times \Delta\kappa \quad (12)$$

and

$$P_{\mathrm{MH}} = \sum_{i=1}^{X} P_{i,\mathrm{MH}} \times c(\kappa)_i \times \Delta\kappa. \tag{13}$$

Thirdly, the per-particle species diversity (D_i), the average per-particle species diversity (D_α) and the population species diversity (D_γ) can be calculated as

$$D_i = e^{H_i}, \tag{14}$$

$$D_\alpha = e^{H_\alpha}, \tag{15}$$

and

$$D_\gamma = e^{H_\gamma}. \tag{16}$$

Finally, a hygroscopic heterogeneity parameter χ can be calculated as

$$\chi = \frac{D_\alpha - 1}{D_\gamma - 1}, \tag{17}$$

which varied from 0% that all particles in the population purely consist of the LH or MH component, to 100% that the LH and MH components are homogeneously distributed ~~in~~ across all particles in the population with identical volume fractions.

2.4 Calculation of the size-resolved heterogeneity

A typical four-mode (i. e., a nucleation mode, an Aitken mode, an accumulation mode and a coarse mode) PNSD with a wide size range of 3 nm-10 μm obtained by Ma (2013) is used for the calculation and presentation of the size-resolved heterogeneity. According to the assumption that ~~aerosols~~ aerosol particles in a specific mode have common sources or have experienced similar ~~ageing~~ aging processes, the corresponding ~~κ_{mean}~~ κ_{mean} and κ-PDF of one mode should be the same. The campaign average ~~κ_{mean}~~ κ_{mean} and κ-PDF for particles with diameters of 40 nm, 80 nm, and 200 nm measured by H-TDMA are used to deduce the respective ~~κ_{mean}~~ κ_{mean} and κ-PDF for the nucleation mode, Aitken mode, and accumulation mode of the fitted PNSDs. Although the primary chemical compositions in the coarse mode aerosol are nearly hydrophobic, some studies showed that this aerosol is slightly hygroscopic due to the coating in atmospheric aging processes (Hegg et al., 2006; Massling et al., 2009; Liu et al., 2014). However, κ for the coarse mode ~~is~~ aerosol is hard to be observed by H-TDMA technique so far, due to the technical bottleneck. Considering that this aerosol has limited influence on radiative forcing and cloud because of its short lifetime and low number concentration, κ for this aerosol is assumed to be 0 ~~because~~

~~the primary chemical composition in this mode is nearly hydrophobic.Considering~~ as Chen et al. (2012) set. According to the contribution of each mode to the ~~κ_{mean}~~ κ_{mean} of specific particle size, the size-resolved ~~κ_{mean} for aerosols~~ κ_{mean} for aerosol particles ranging from 3 nm-10 μm can be estimated from the known ~~κ_{mean}~~ κ_{mean} of each mode ($\kappa_{\mathrm{mean},i}$) as:

$$\kappa_{\mathrm{mean}}(D_{\mathrm{p}}) = \frac{\sum_{i=1}^{4} \kappa_{\mathrm{mean},i} \times N_i(D_{\mathrm{p}})}{\sum_{i=1}^{4} N_i(D_{\mathrm{p}})}. \tag{18}$$

The size-resolved κ-PDF can be calculated using the similar method with Eq. 19:

$$c(\kappa, (D_{\mathrm{p}}) = \frac{\sum_{i=1}^{4} c(\kappa, i) \times \Delta\kappa \times N_i(D_{\mathrm{p}})}{\sum_{i=1}^{4} N_i(D_{\mathrm{p}}) \times \Delta\kappa \times \Delta \log D_{\mathrm{p}}} \frac{\sum_{i=1}^{4} N_i(D_{\mathrm{p}}) \times c(\kappa)_i \times \Delta\kappa}{\sum_{i=1}^{4} N_i(D_{\mathrm{p}}) \times \Delta\kappa \times \Delta \log D_{\mathrm{p}}}. \tag{19}$$

~~Thus~~Then, the size-resolved heterogeneity $D_\alpha(D_{\mathrm{p}})$, $D_\gamma(D_{\mathrm{p}})$, and $\chi(D_{\mathrm{p}})$ for the wide range of 3 nm -10 μm can be obtained by using Eqs. 5-17.

3 Results

3.1 Diagram for particle-to-particle heterogeneity in aerosol hygroscopicity

From the calculation of Eqs. 15-17, D_α can represent the average of the effective number of species existing in each particle and D_γ can represent the effective number of species in the population. Note that $1 \leq D_\alpha \leq D_\gamma$. D_α = 1 when all particles are pure while $D_\alpha = D_\gamma$ when all aerosol particles have identical components. The value of D_γ ranges from 1 to 2 according to the volume ratio of the LH and MH components in the population. Specifically, it is 1 when the population purely consists of the LH or MH component while is 2 when the population has the equivalent volume of the LH and MH components. A triangular region is thus presented in Fig. 2, in which χ is represented by contours~~and varies from 0% (all particles in the population purely consisted of the LH or MH component, Fig. 2a) to 100% (the LH and MH components are homogeneously distributed in all particles in the population with identical volume fractions, Fig. 2d)~~.

Figs. 2a-2d show an example of the evolution of the heterogeneity in aerosol hygroscopicity. The distributions of the NH and MH components vary between and within populations, causing different heterogeneities for these ~~aerosol populations~~aerosols. Twelve red dots in Fig. 2e represent ~~aerosol populations~~aerosols, each consisting of six aerosol particles with varied fractions of the LH and MH components. Their respective sketch maps and heterogeneity indices are summarized in Table 1, and the corresponding κ-PDFs are listed in Fig. S3 in the supplemental file.

For ~~aerosol populations~~ aerosols with particles purely consisting of the LH component or MH component ~~,~~ (e.g., populations 1-4 ~~,~~ in Fig. 2e and Table 1), D_α equals 1 and χ equals 0, although D_γ varies from 1 to 2 due to the change of the bulk volume ratio of the LH and MH components. Their κ-PDFs show that κ distributes only at 0.01 for the LH component or 0.6 for the MH component due to the pure component in each particle.

For ~~aerosol populations~~ aerosols with equal bulk volume fractions of the LH and MH components ~~,~~ (e.g., populations 4-7 and populations ~~12-10, D_γ has~~ 10-12 in Fig. 2e and Table 1), D_γ have constant values of 2 and 1.5, respectively. ~~The heterogeneous~~

distribution However, the different distributions of the LH and MH components contributes to relatively dispersive κ-PDF, with lower D_α in each particle of an aerosol contribute to different D_α and χ. While the homogeneous distribution of these two components, in which all particles have equal amounts of the LH and MH components, leads to a very Specifically, the heterogeneous distribution (e.g., populations 4-6 and populations 11-12 in Fig. 2e and Table 1) leads to relatively small values of D_α and χ, and the dispersed κ-PDF. On the contrary, the homogeneous distribution (e.g., populations 7 and 10 in Fig. 2e and Table 1) generates a narrow κ-PDF, and thus higher D_α relatively high D_α and χ.

For aerosol populations aerosols consisting of particles with identical volume fractions , of the LH and MH components (e.g., populations 7-10 , in Fig. 2e and Table 1), equal values of D_α and D_γ D_α and D_χ for each population result in χ of 1, although the bulk ratio of the LH to MH components changes between populations. Accordingly, their κ-PDFs are concentrated at a single value of $\kappa_{\rm mean}$ $\kappa_{\rm mean}$.

From the populations, it can be concluded that the particle-to-particle heterogeneity in hygroscopicity resulting from the distribution discrepancy of the LH and MH components within particles can be quantified according to the κ-PDF using the proposed algorithm of this work, which which is of importance to the further analysis of the existing κ-PDF and can help the heterogeneity to be considered in the calculation of aerosol climate-relevant properties.

3.2 Evolution of the heterogeneity in the real atmosphere

In this section, we apply applied the proposed algorithm to the in-situ measurement of H-TDMA that was implemented for two periods in 2019 located in Chengdu, Chinaand show the variation characteristic of D_α, D_γ, and χ in the real atmosphere. In the following, the expression of the κ-PDF is equivalent to the probability distribution function of g (g-PDF) due to their one-to-one corresponding relationship. Two In order to show the variation characteristics and the significance of D_α, D_γ, and χ in the real atmosphere, especially for the condition that the total hygroscopicity of aerosol remained constant, two episodes with tiny changes of $\kappa_{\rm mean}$ change of $\kappa_{\rm mean}$ during the observation periods , showing are presented. The 110 nm aerosol is chosen as the example to show the typical evolution processes for aerosol heterogeneity, because it has large number concentration and lies in the transition zone between the diameters that show the processes of gas to particle (<100 nm) and aging (>100 nm) in the atmosphere. The variation of the heterogeneity in 110 nm aerosol populations are chosen and shown in Fig. 3.nm aerosol can better reflect the evolution of aerosol particles in the real atmosphere and may have a great impact on the direct radiative forcing. The first episode appeared from 22:00 (LST) January 1323, 2019 to 08:00 (LST) January 1424, 2019, and the other one occurred from 00:00 January 27, 2019 to 12:00 January 27, 2019. These two episodes showed The variations of D_α, D_γ, χ, and $\kappa_{\rm mean}$ during these two episodes are shown in Fig. 3. The tiny change of $\kappa_{\rm mean}$ indicates the slight variation of the bulk fraction of the LH and MH components in the aerosol. The decreasing trends of D_α and χ reveal that the existing aged aerosol populations with unimodal distributions of κ-PDF, which indicate the aerosols with uniformly distributed LH and MH components among particles and thus at night, indicated by the unimodal distributions of κ-PDF and relatively high χ (0.831 for episode 1 at 22:00 and 0.832 for episode 2 at 00:00), were intruded by the fresh emissions during the night midnight as reflected by the bimodal and wider distribution of κ-PDF (Yuan et al., 2020). This process led to component discrepancies among particles in populations and thus the decrease of D_α D_α and χ during the midnight.

The statistical PDF of ~~D_α, D_γ~~ D_α, D_γ, and χ for aerosols with five measured diameters are shown in Fig. 4. The patterns of the distributions for ~~D_α and D_γ~~ D_α and D_γ move to larger values with increasing diameter, indicating that the effective number of species increases in aerosols with larger diameter due to the longer aging time in the atmosphere. This trend is more obvious in summer campaign. Taking the ~~aerosols~~ aerosol of 110 nm for example, ~~D_α~~ D_α varies between 1.386 and 1.850, and ~~D_γ~~ D_γ varies between 1.470 and 2.000 during the winter field measurements. The ranges of ~~D_α and D_γ~~ D_α and D_γ in summer are 1.280-1.928 and 1.371-2.000, respectively, contributing to a wider distribution of χ. This indicates that the fraction of the LH and MH components varied more pronounced due to the more complex aging processes in summer compared to that in winter. χ ranging from 0.6 to 0.9 reveals the large variation of heterogeneity in aerosol hygroscopicity in the real atmosphere.

~~In short, the~~ The details in the variation characteristics of the heterogeneity and the difference among the aerosols of five measured diameters will be further discussed in our future studies. It can be concluded from the discussion above, aerosols with tiny variation of $\kappa_{\rm mean}$ can have ever-changing heterogeneity in aerosol hygroscopicity in the atmosphere. The algorithm proposed in this work can efficiently characterize ~~the evolution of aerosol~~ this heterogeneity with time ~~in the real atmosphere and provides~~ and provide detail information about the evolution of aerosols in the air. More importantly, this algorithm offers an unexplored understanding of the H-TDMA measurement.

3.3 Importance of the heterogeneity in aerosol hygroscopicity

The same bulk volume fraction of the LH and MH components indicates the same ~~$\kappa_{\rm mean}$~~ $\kappa_{\rm mean}$ for populations (e.g., populations 4-7 and populations 10-12). This reveals the identical diameter for all particles in each population after hygroscopic growth at high RH. Actually, due to the particle-to-particle heterogeneity in one population, different ratios of the LH and MH components in each particle result in different κ (e.g., particles in each of populations 4-7), which can lead to different ambient number size distributions, especially for the condition with high RH. Fig. 5 depicts a sample of the hygroscopic size distribution, where RH is 90%, for three ~~aerosol populations~~ aerosols with the same ~~$\kappa_{\rm mean}$~~ $\kappa_{\rm mean}$ of 0.305 but different χ of 0.653, 0.884, and 0.999, respectively. Each of these three populations contains 1000 aerosol particles with dry diameters of 100 nm. Significant discrepancies can be seen in the number size distribution that the width decreases while the peak value increases with increasing χ after hygroscopic growth. Thus, the heterogeneity in aerosol hygroscopicity plays a significant role in the evolution of aerosol ambient number size distributions, which is a key factor for evaluating aerosol radiative forcing.

3.4 Size-resolved heterogeneity in aerosol hygroscopicity

The heterogeneity for only one size can contribute to dramatically different ambient size distributions, especially for the condition under high RH. Thus, it is urgently needed to figure out how the heterogeneity varies with aerosol size in the real atmosphere. This section ~~will discuss~~ discussed the characteristic of the size-resolved heterogeneity in aerosol hygroscopicity.

The PNSD within the range of 3 nm-10 μm is commonly observed by commercial instruments, including the scanning mobility particle sizer (SMPS) and the Wide Range Particle Spectrometer (WPS) around the world (Wu and Boor, 2021). However, the widely used H-TDMA technic can only observe the growth factor of aerosols with limited sizes (generally smaller than 350 nm in the dry condition), e.g., 40, 80, 110, 150, and 200 nm in this study. Recently, Shen et al. (2021) ex-

tended the H-TDMA measurement of aerosol hygroscopic properties to 600 nm in the urban environment. Although κ for larger particles (> 1 μm) can be derived from the size-resolved chemical composition ~~(Liu et al., 2014; Gysel et al., 2007)~~ (Gysel et al., 2007; Liu et al., 2014), the size-resolved κ with high size and time resolution is scarce and is needed to be observed or reversed by more advanced technology and new algorithms. Fortunately, Chen et al. (2012) provided an approach to derive the size-resolved κ for aerosols within the range of 3 nm-10 μm based on the measured PNSDs and H-TDMA determined κ. They used the ~~κ_{mean}~~ κ_{mean} for each measured size by neglecting aerosol heterogeneity. Here, the heterogeneity in aerosol hygroscopicity is considered based on the method provided by Chen et al. (2012)~~(Methods section)~~.

The typical four-mode PNSD mentioned above is used and shown in Fig. 6a and Fig. 6d. The ~~κ_{mean}~~ κ_{mean} and the corresponding κ-PDFs for the nucleation mode, Aitken mode, and accumulation mode are represented by those measured at sizes of 40 nm, 80 nm, and 200 nm, respectively, during the winter (Fig. 6b) and summer (Fig. 6e) campaigns. The calculated size-resolved ~~κ_{mean}~~ κ_{mean} are shown in Fig. 6c (winter) and Fig. 6f (summer), in which κ-PDF for each size contributed by the heterogeneity in aerosol hygroscopicity is represented by the contour. The variation of both the size-resolved ~~κ_{mean}~~ κ_{mean} and the corresponding κ-PDF are influenced by the contribution of each mode to the total number concentration. The corresponding χ for the size range of 3 nm-10 μm can therefore be calculated by using the framework proposed by this work.

As shown in Fig. 6, the consideration of the heterogeneity provides the size-resolved κ-PDF, which can further show the region where the κ is mostly distributed for ~~aerosol populations~~ aerosols of any size and how ~~aerosols~~ aerosol particles evolve with size in the population. For example, although ~~κ_{mean} for aerosol populations~~ the κ_{mean} for aerosols smaller than 40 nm is 0.131 during the winter campaign, the κ-PDF shows most κ locate at a narrow area lower than 0.05. The continuous evolution of the κ-PDF with sizes smaller than 1 μm indicates that on the one hand, a part of the ~~aerosols~~ aerosol particles in the population has increasing hygroscopicity during the aging process of growing up, which is the main reason for the increase of ~~κ_{mean}~~ κ_{mean}, on the other hand, NH-dominated ~~aerosols~~ particles exist across all sizes. This corresponds to the slight decreasing trend of χ accompanied by a wider area of κ ranging from 0.01 to larger than 0.4, which reflects the heterogeneous distribution of the LH and MH components between aerosol particles within a population during the aging progress.

Additionally, the phenomenon that a sharp decrease of χ close to 0.1 for ~~aerosol populations~~ aerosols larger than 1 μm and the κ-PDFs for this size range shows a very narrow band lying at κ of 0 responds to the assumption that the coarse mode particle is mainly composed of the NH component.

Overall, this newly developed aerosol heterogeneity provides more insight into the evolution of ~~aerosol populations~~ aerosols during the aging processes. The hygroscopicity of an ~~aerosol population~~ aerosol is complicated and diverse due to the particle-to-particle heterogeneity in aerosol hygroscopicity, if only the ~~κ_{mean}~~ κ_{mean} is applied without considering aerosol heterogeneity, significant uncertainty will occur.

4 Conclusions

The particle-to-particle heterogeneity in aerosol hygroscopicity is of great importance for better understanding the impact of hygroscopicity on estimating aerosol climatic and environmental effects. Unfortunately, the heterogeneity has not been paid

attention to in previous studies, of which only the population-averaged hygroscopicity parameter, ~~κ_{mean}~~ κ_{mean}, is considered, mainly because the heterogeneity is difficult to be quantified in both observations and models.

In this work, we proposed an algorithm to quantify the particle-to-particle heterogeneity in aerosol hygroscopicity from the in-situ measurement for the first time. This algorithm is an innovation on the basis of the mature theory in information-theoretic entropy and the widely used assumption that ~~aerosol populations~~ aerosols are binary systems consisting of the commonly defined LH and MH components from H-TDMA measurement.

Three indices, including the average per-particle species diversity D_α, the bulk population species diversity D_γ , and their affine ratio χ, are calculated from the probability distribution of κ to together describe aerosol heterogeneity. They can efficiently characterize and provide more insight into the evolution of aerosol heterogeneity with time in the real atmosphere during the aging processes.

The heterogeneity varies much with aerosol particle size and large discrepancies can be seen in aerosol particle number size distribution (PNSD) that the width decreases while the peak value of the PNSD increases with increasing χ after hygroscopic growth, especially for conditions with high relative humidity, indicating the vital role of the heterogeniety in the evolution of ambient PNSD.

Considering that PNSD is a key factor for the evaluation of aerosol impacts on radiative forcing, significant uncertainties will occur in calculating the climate-relevant properties if ~~the population-averaged hygroscopicity~~ κ_{mean} is applied by neglecting its heterogeneity. Thus, the particle-to-particle heterogeneity in aerosol hygroscopicity is urgently needed to be represented in models. ~~This~~ The algorithm proposed by this work, which has the intuitive and quantitative interpretation of aerosol heterogeneity, sheds light on the ~~importance and provides a framework of merging observations into~~ reanalysis of the existing H-TDMA datasets and could have a large impact on how we use and think about these datasets. It can also provide a bridge for using observations to constrain numerical models to deeply investigate how heterogeneity in aerosol hygroscopicity influences aerosol effects on climate and environment.

Data availability. The data is available at https://doi.org/10.5281/zenodo.7320916.

Author contributions. C.Z. designed the research project and reviewed the manuscript. L.Y. interpreted all results and contributed to writing.

Competing interests. The authors declare no competing interests.

Acknowledgements. The authors acknowledge Dr. Yuzhang Che, Prof. Pengguo Zhao, ~~Jinhui,~~ Dr. Jinhui Gao, and Dr. Hui Xiao for fruitful discussions. This work is supported by the National Science Foundation of China (NSFC) (42275070, 42005072, and 42075086) and the Open Project of Key Laboratory for Aerosol-Cloud-Precipitation of China Meteorological Administration, NUIST (KDW1903).

References

Bian, Y., Zhao, C., Ma, N., Chen, J., and Xu, W.: A study of aerosol liquid water content based on hygroscopicity measurements at high relative humidity in the North China Plain, Atmospheric Chemistry and Physics, 14, 6417–6426, https://doi.org/10.5194/acp-14-6417-2014, 2014.

Brock, C. A., Wagner, N. L., Anderson, B. E., Attwood, A. R., Beyersdorf, A., Campuzano-Jost, P., Carlton, A. G., Day, D. A., Diskin, G. S., Gordon, T. D., et al.: Aerosol optical properties in the southeastern United States in summer–Part 1: Hygroscopic growth, Atmospheric Chemistry and Physics, 16, 4987–5007, https://doi.org/10.5194/acp-16-4987-2016, 2016.

Cai, M., Tan, H., Chan, C. K., Qin, Y., Xu, H., Li, F., Schurman, M. I., Liu, L., and Zhao, J.: The size-resolved cloud condensation nuclei (CCN) activity and its prediction based on aerosol hygroscopicity and composition in the Pearl Delta River (PRD) region during wintertime 2014, Atmospheric Chemistry and Physics, 18, 16 419–16 437, https://doi.org/10.5194/acp-18-16419-2018, 2018.

Chen, J., Zhao, C., Ma, N., Liu, P., Göbel, T., Hallbauer, E., Deng, Z., Ran, L., Xu, W., Liang, Z., et al.: A parameterization of low visibilities for hazy days in the North China Plain, Atmospheric Chemistry and Physics, 12, 4935–4950, https://doi.org/10.5194/acp-12-4935-2012, 2012.

Chen, J., Zhao, C., Ma, N., and Yan, P.: Aerosol hygroscopicity parameter derived from the light scattering enhancement factor measurements in the North China Plain, Atmospheric Chemistry and Physics, 14, 8105–8118, https://doi.org/10.5194/acp-14-8105-2014, 2014.

Drucker, J.: Industrial structure and the sources of agglomeration economies: evidence from manufacturing plant production, Growth and Change, 44, 54–91, https://doi.org/10.1111/grow.12002, 2013.

Falush, D., Stephens, M., and Pritchard, J. K.: Inference of population structure using multilocus genotype data: dominant markers and null alleles, Molecular ecology notes, 7, 574–578, https://doi.org/10.1111/j.1471-8286.2007.01758.x, 2007.

Fierce, L., Bond, T. C., Bauer, S. E., Mena, F., and Riemer, N.: Black carbon absorption at the global scale is affected by particle-scale diversity in composition, Nature communications, 7, 1–8, https://doi.org/10.1038/ncomms12361, 2016.

Fierce, L., Onasch, T. B., Cappa, C. D., Mazzoleni, C., China, S., Bhandari, J., Davidovits, P., Fischer, D. A., Helgestad, T., Lambe, A. T., et al.: Radiative absorption enhancements by black carbon controlled by particle-to-particle heterogeneity in composition, Proceedings of the National Academy of Sciences, 117, 5196–5203, https://doi.org/10.1073/pnas.1919723117, 2020.

Gysel, M., Crosier, J., Topping, D., Whitehead, J., Bower, K., Cubison, M., Williams, P., Flynn, M., McFiggans, G., and Coe, H.: Closure study between chemical composition and hygroscopic growth of aerosol particles during TORCH2, Atmospheric Chemistry and Physics, 7, 6131–6144, https://doi.org/10.5194/acp-7-6131-2007, 2007.

Gysel, M., McFiggans, G., and Coe, H.: Inversion of tandem differential mobility analyser (TDMA) measurements, Journal of Aerosol Science, 40, 134–151, https://doi.org/10.1016/j.jaerosci.2008.07.013, 2009.

Hegg, D., Covert, D. S., Crahan, K., Jonsson, H., and Liu, Y.: Measurements of aerosol size-resolved hygroscopicity at sub and supermicron sizes, Geophysical research letters, 33, L21 808, https://doi.org/10.1029/2006GL026747, 2006.

Köhler, H.: The nucleus in and the growth of hygroscopic droplets, Transactions of the Faraday Society, 32, 1152–1161, https://doi.org/10.1039/tf9363201152, 1936.

Kuang, Y., Zhao, C., Tao, J., Bian, Y., Ma, N., and Zhao, G.: A novel method for deriving the aerosol hygroscopicity parameter based only on measurements from a humidified nephelometer system, Atmospheric Chemistry and Physics, 17, 6651–6662, https://doi.org/10.5194/acp-17-6651-2017, 2017.

Li, W., Teng, X., Chen, X., Liu, L., Xu, L., Zhang, J., Wang, Y., Zhang, Y., and Shi, Z.: Organic coating reduces hygroscopic growth of phase-separated aerosol particles, Environmental Science & Technology, 55, 16 339–16 346, https://doi.org/10.1021/acs.est.1c05901, 2021.

Liu, B., Pui, D., Whitby, K., Kittelson, D. B., Kousaka, Y., and McKenzie, R.: The aerosol mobility chromatograph: a new detector for sulfuric acid aerosols, Atmospheric Environment, pp. 99–104, https://doi.org/10.1016/0004-6981(78)90192-0, 1978.

Liu, H., Zhao, C., Nekat, B., Ma, N., Wiedensohler, A., Van Pinxteren, D., Spindler, G., Müller, K., and Herrmann, H.: Aerosol hygroscopicity derived from size-segregated chemical composition and its parameterization in the North China Plain, Atmospheric Chemistry and Physics, 14, 2525–2539, https://doi.org/10.5194/acp-14-2525-2014, 2014.

Liu, P., Zhao, C., Göbel, T., Hallbauer, E., Nowak, A., Ran, L., Xu, W., Deng, Z., Ma, N., Mildenberger, K., et al.: Hygroscopic properties of aerosol particles at high relative humidity and their diurnal variations in the North China Plain, Atmospheric Chemistry and Physics, 11, 3479–3494, https://doi.org/10.5194/acp-11-3479-2011, 2011.

Liu, X. G., Li, J., Qu, Y., Han, T., Hou, L., Gu, J., Chen, C., Yang, Y., Liu, X., Yang, T., Zhang, Y., Tian, H., and Hu, M.: Formation and evolution mechanism of regional haze: a case study in the megacity Beijing, China, Atmospheric Chemistry and Physics, 13, 4501–4514, https://doi.org/10.5194/acp-13-4501-2013, 2013.

Ma, N.: Aerosol optical and activation properties in the North China Plain, Peking University, 2013.

Massling, A., Stock, M., Wehner, B., Wu, Z., Hu, M., Brüggemann, E., Gnauk, T., Herrmann, H., and Wiedensohler, A.: Size segregated water uptake of the urban submicrometer aerosol in Beijing, Atmospheric Environment, 43, 1578–1589, https://doi.org/10.1016/j.atmosenv.2008.06.003, 2009.

Pang, Y., Wang, Y., Wang, Z., Zhang, Y., Liu, L., Kong, S., Liu, F., Shi, Z., and Li, W.: Quantifying the fractal dimension and morphology of individual atmospheric soot aggregates, Journal of Geophysical Research: Atmospheres, 127, e2021JD036 055, https://doi.org/10.1029/2021JD036055, 2022.

Petters, M. and Kreidenweis, S.: A single parameter representation of hygroscopic growth and cloud condensation nucleus activity, Atmospheric Chemistry and Physics, 7, 1961–1971, https://doi.org/10.5194/acp-7-1961-2007, 2007.

Riemer, N. and West, M.: Quantifying aerosol mixing state with entropy and diversity measures, Atmospheric Chemistry and Physics, 13, 11 423–11 439, https://doi.org/10.5194/acp-13-11423-2013, 2013.

Shen, C., Zhao, G., Zhao, W., Tian, P., and Zhao, C.: Measurement report: aerosol hygroscopic properties extended to 600 nm in the urban environment, Atmospheric Chemistry and Physics, 21, 1375–1388, https://doi.org/10.5194/acp-21-1375-2021, 2021.

Stokes, R. and Robinson, R.: Interactions in aqueous nonelectrolyte solutions. I. Solute-solvent equilibria, The Journal of Physical Chemistry, 70, 2126–2131, https://doi.org/10.1021/j100879a010, 1966.

Stolzenburg, M. R. and McMurry, P. H.: Equations governing single and tandem DMA configurations and a new lognormal approximation to the transfer function, Aerosol Science and Technology, 42, 421–432, https://doi.org/10.1080/02786820802157823, 2008.

Strong, S. P., Koberle, R., Van Steveninck, R. R. D. R., and Bialek, W.: Entropy and information in neural spike trains, Physical review letters, 80, 197, https://doi.org/10.1103/PhysRevLett.80.197, 1998.

Su, H., Rose, D., Cheng, Y., Gunthe, S., Massling, A., Stock, M., Wiedensohler, A., Andreae, M., and Pöschl, U.: Hygroscopicity distribution concept for measurement data analysis and modeling of aerosol particle mixing state with regard to hygroscopic growth and CCN activation, Atmospheric Chemistry and Physics, 10, 7489–7503, https://doi.org/10.5194/acp-10-7489-2010, 2010.

Swietlicki, E., Hansson, H.-C., Hämeri, K., Svenningsson, B., Massling, A., McFiggans, G., McMurry, P., Petäjä, T., Tunved, P., Gysel, M., et al.: Hygroscopic properties of submicrometer atmospheric aerosol particles measured with H-TDMA instruments in various en-

vironments—a review, Tellus B: Chemical and Physical Meteorology, 60, 432–469, https://doi.org/10.1111/j.1600-0889.2008.00350.x, 2008.

Tan, H., Xu, H., Wan, Q., Li, F., Deng, X., Chan, P., Xia, D., and Yin, Y.: Design and application of an unattended multifunctional H-TDMA system, Journal of Atmospheric and Oceanic Technology, 30, 1136–1148, https://doi.org/10.1175/JTECH-D-12-00129.1, 2013a.

Tan, H., Yin, Y., Gu, X., Li, F., Chan, P., Xu, H., Deng, X., and Wan, Q.: An observational study of the hygroscopic properties of aerosols over the Pearl River Delta region, Atmospheric Environment, 77, 817–826, https://doi.org/10.1016/j.atmosenv.2013.05.049, 2013b.

Tao, J., Zhao, C., Ma, N., and Liu, P.: The impact of aerosol hygroscopic growth on the single-scattering albedo and its application on the NO_2 photolysis rate coefficient, Atmospheric Chemistry and Physics, 14, 12 055–12 067, https://doi.org/10.5194/acp-14-12055-2014, 2014.

Tie, X., Huang, R.-J., Cao, J., Zhang, Q., Cheng, Y., Su, H., Chang, D., Pöschl, U., Hoffmann, T., Dusek, U., et al.: Severe pollution in China amplified by atmospheric moisture, Scientific Reports, 7, 1–8, https://doi.org/10.1038/s41598-017-15909-1, 2017.

Tsimring, L. S., Levine, H., and Kessler, D. A.: RNA virus evolution via a fitness-space model, Physical review letters, 76, 4440, https://doi.org/10.1103/PhysRevLett.76.4440, 1996.

Wang, Y. and Chen, Y.: Significant climate impact of highly hygroscopic atmospheric aerosols in Delhi, India, Geophysical Research Letters, 46, 5535–5545, https://doi.org/10.1029/2019GL082339, 2019.

Wang, Y., Li, Z., Zhang, Y., Du, W., Zhang, F., Tan, H., Xu, H., Fan, T., Jin, X., Fan, X., et al.: Characterization of aerosol hygroscopicity, mixing state, and CCN activity at a suburban site in the central North China Plain, Atmospheric Chemistry and Physics, 18, 11 739–11 752, https://doi.org/10.5194/acp-18-11739-2018, 2018.

Whittaker, R. H.: Evolution and measurement of species diversity, Taxon, 21, 213–251, https://doi.org/10.2307/1218190, 1972.

Wu, T. and Boor, B. E.: Urban aerosol size distributions: a global perspective, Atmospheric Chemistry and Physics, 21, 8883–8914, https://doi.org/10.5194/acp-21-8883-2021, 2021.

Yuan, L., Zhang, X., Feng, M., Liu, X., Che, Y., Xu, H., Schaefer, K., Wang, S., and Zhou, Y.: Size-resolved hygroscopic behaviour and mixing state of submicron aerosols in a megacity of the Sichuan Basin during pollution and fireworks episodes, Atmospheric Environment, 226, 117 393, https://doi.org/10.1016/j.atmosenv.2020.117393, 2020.

Zdanovskii, A.: New methods for calculating solubilities of electrolytes in multicomponent systems, Zh. Fiz. Khim, 22, 1478–1485, 1948.

Zhao, G., Tan, T., Zhu, Y., Hu, M., and Zhao, C.: Method to quantify black carbon aerosol light absorption enhancement with a mixing state index, Atmospheric Chemistry and Physics, 21, 18 055–18 063, https://doi.org/10.5194/acp-21-18055-2021, 2021.

Zheng, Z., West, M., Zhao, L., Ma, P.-L., Liu, X., and Riemer, N.: Quantifying the structural uncertainty of the aerosol mixing state representation in a modal model, Atmospheric Chemistry and Physics, 21, 17 727–17 741, https://doi.org/10.5194/acp-21-17727-2021, 2021.

Zieger, P., Fierz-Schmidhauser, R., Weingartner, E., and Baltensperger, U.: Effects of relative humidity on aerosol light scattering: results from different European sites, Atmospheric Chemistry and Physics, 13, 10 609–10 631, https://doi.org/10.5194/acp-13-10609-2013, 2013.

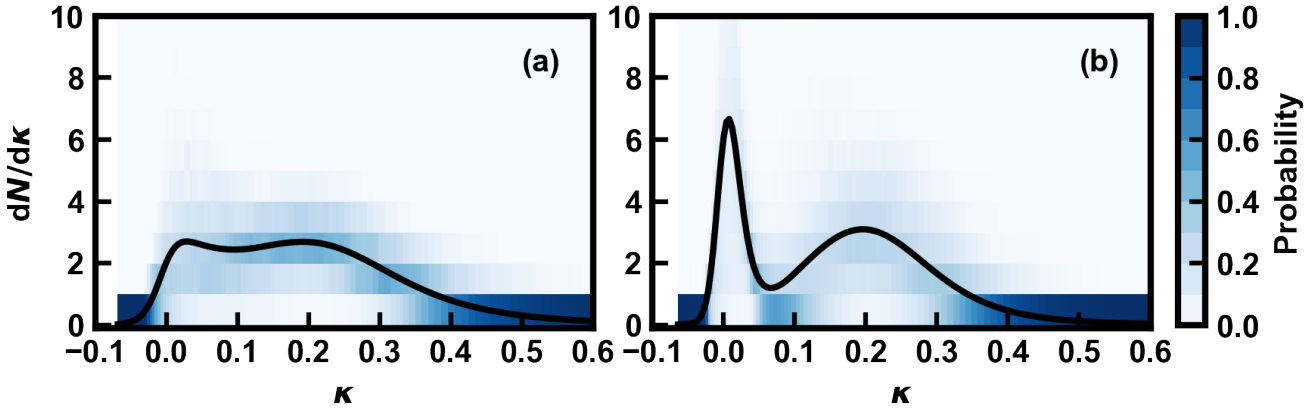

Figure 1. Typical κ-PDF for 100 nm aerosols in winter (a) and summer (b) measured by H-TDMA over Chengdu. The shaded is the frequency distribution of κ-PDF, and the solid lines show the campaign average of κ-PDF.

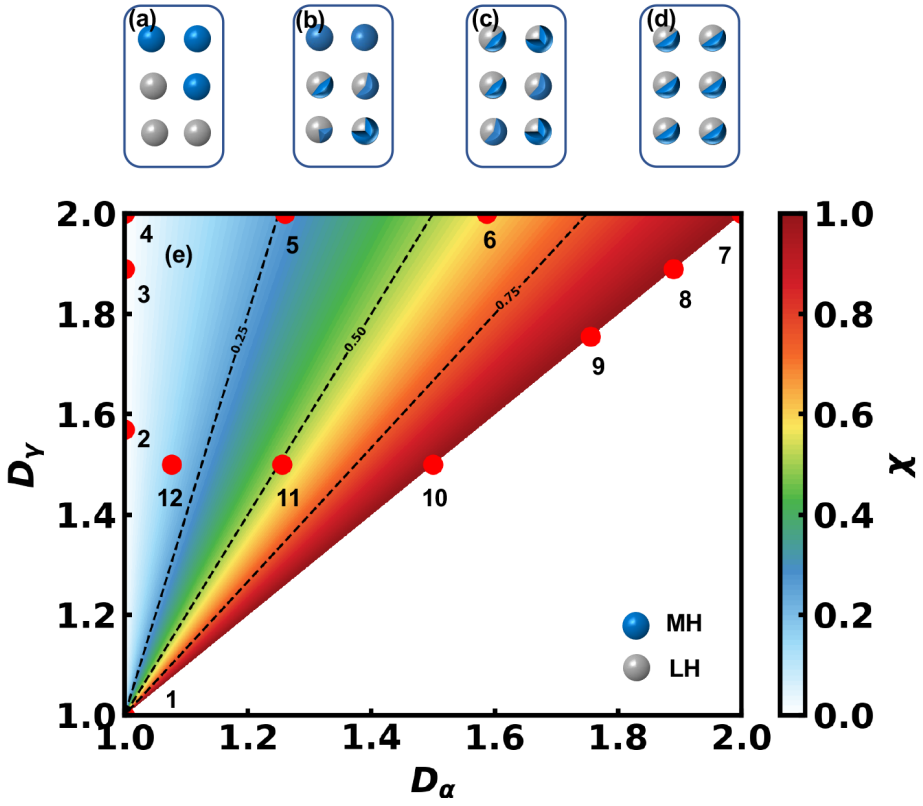

Figure 2. Example of the evolution of the heterogeneity in aerosol hygroscopicity (a-d) and diagram for the relationship among D_α, D_γ, and χ (e). Twelve different ~~aerosol populations~~aerosols, each of which consists of six particles as shown in Table 1, are represented by the red points.

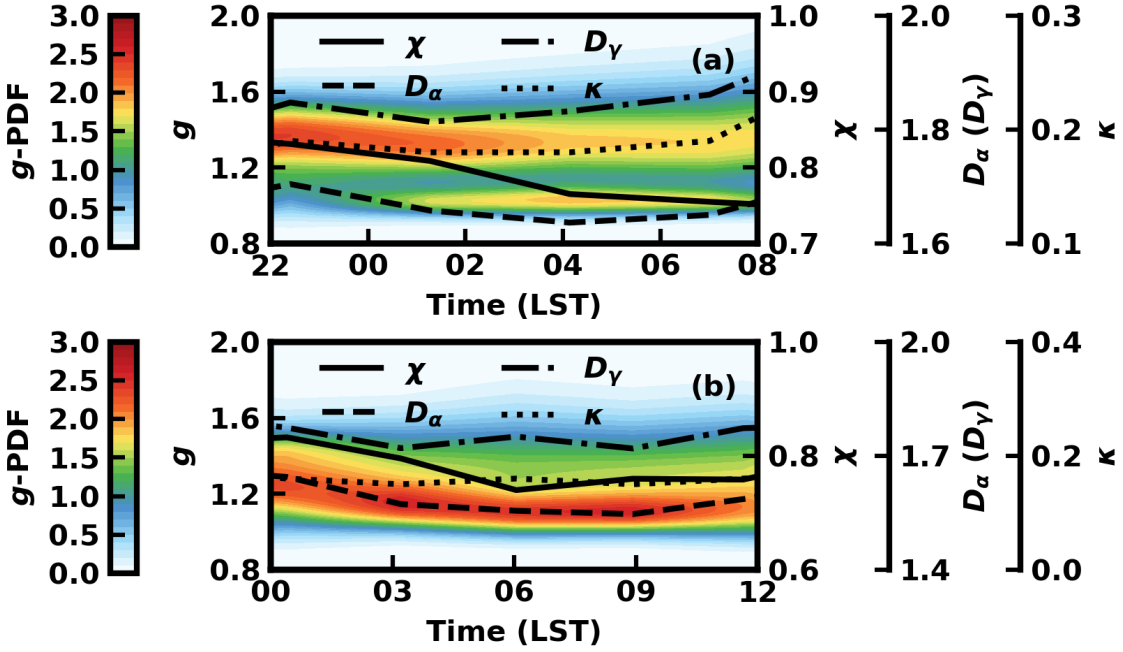

Figure 3. The variation of κ-PDF, D_α, D_γ, and χ during two typical evolution processes for 110 nm ~~aerosol populations~~ aerosols with tiny changes of ~~κ_{mean}~~ κ_{mean} on January ~~13~~23, 2019 (a) and January 27, 2019 (b).

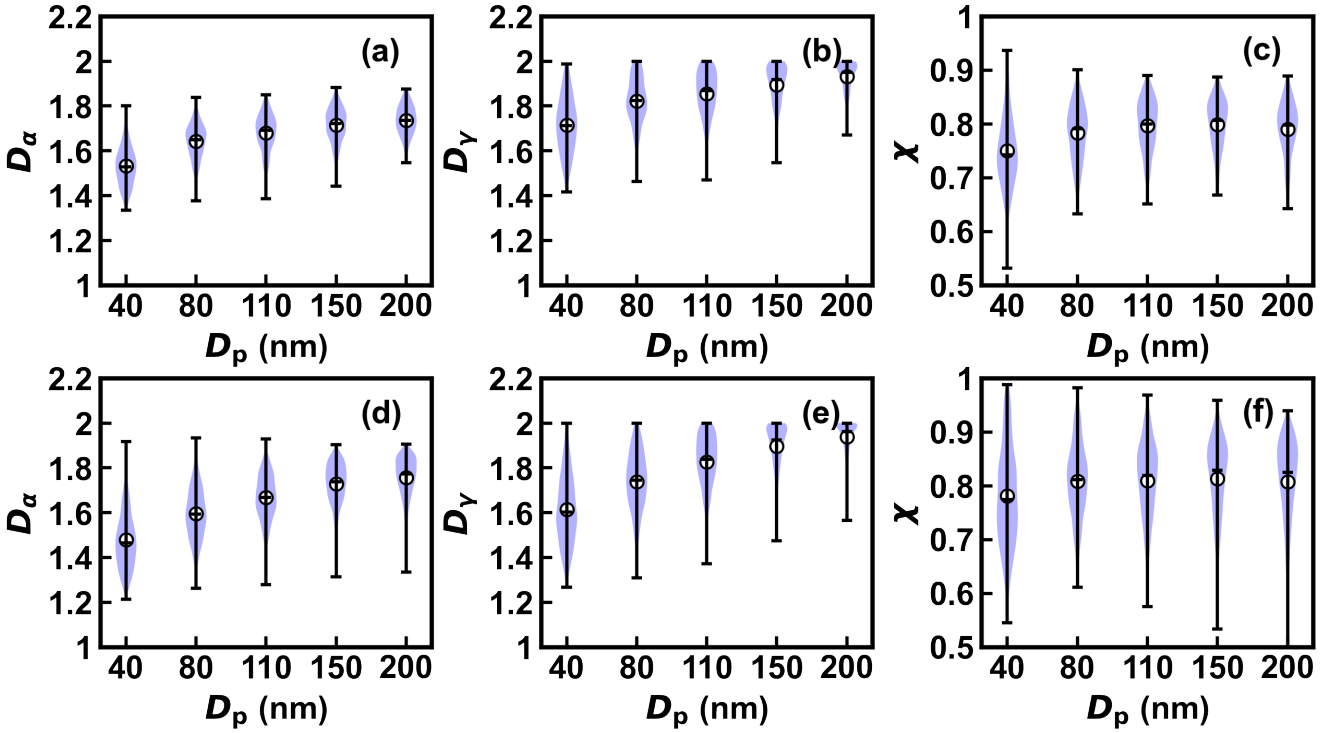

Figure 4. The statistical of ~~D_α~~ D_α, ~~D_γ~~ D_γ, and χ for ~~aerosol populations~~ aerosols of five measured diameters in winter (a), (b), (c) and summer (d), (e), (f). The shaded is the frequency distribution of the indices. The three bars on whisker for each diameter from the bottom to the top are the minimum, median, and maxmum, and the circles represent the average of the indices.

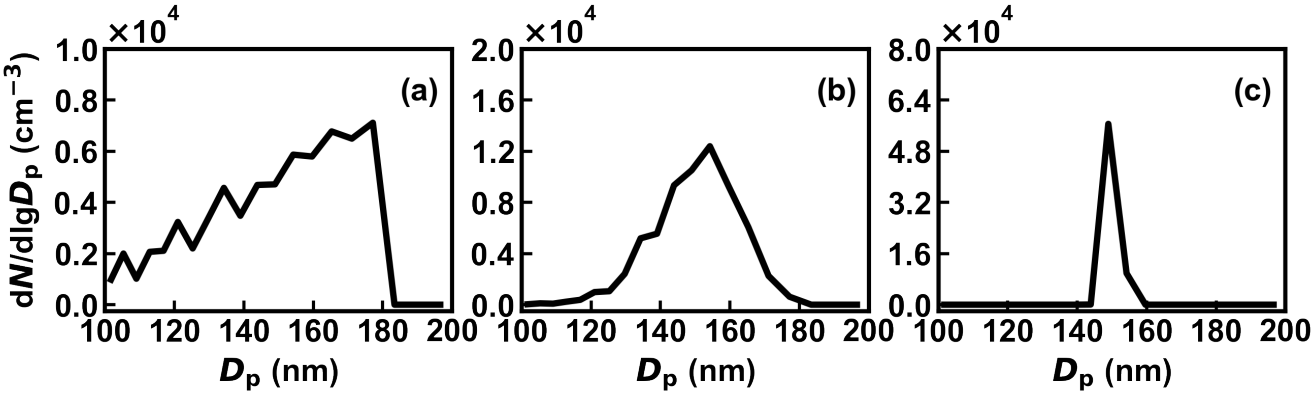

Figure 5. Aerosol particle size distributions after hygroscopic growth at RH of 90% for three ~~aerosol populations~~ aerosols with χ of 0.653 (a), 0.884 (b), and 1 (c), respectively. Each of these three populations has the same κ_{mean} of 0.305 and contains 1000 aerosol particles with dry diameters of 100 nm.

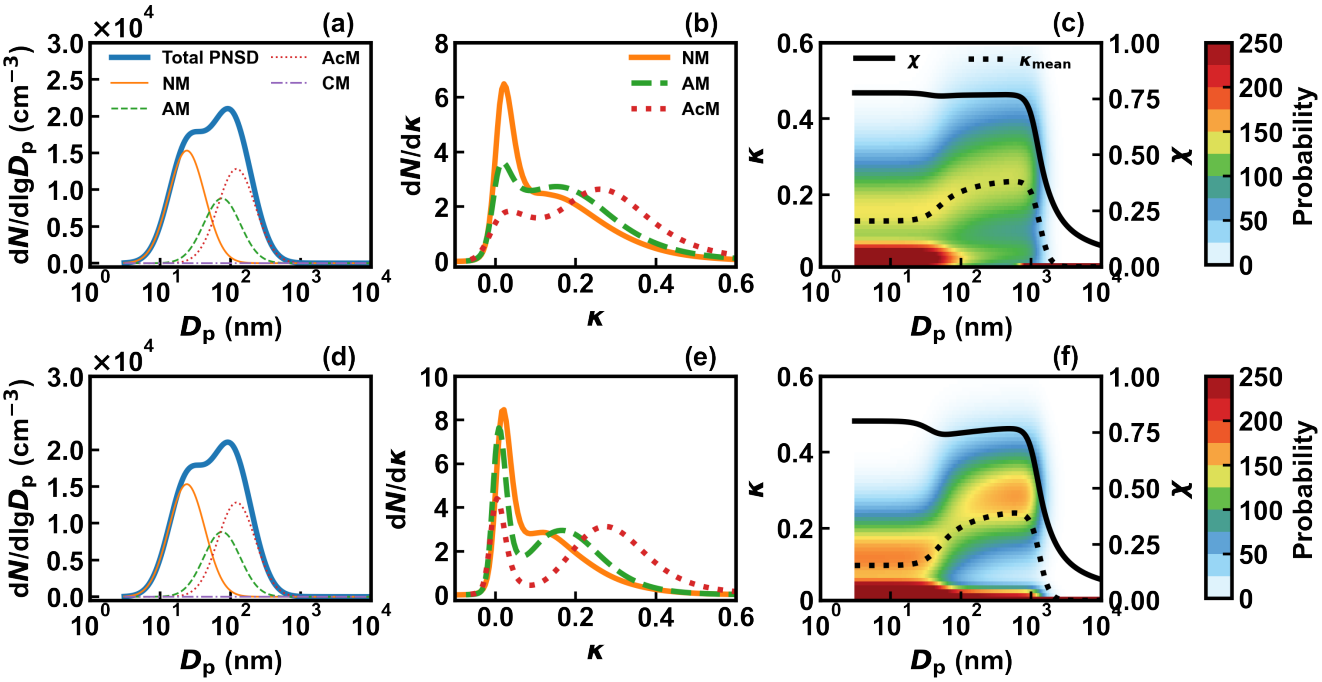

Figure 6. The typical PNSD (a), (d) and the κ-PDF during the winter (b) and summer campaigns (e) used for calculating the size-resolve ~~κ_{mean}~~κ_{mean}, the size-resolved κ-PDF, and the corresponding size-resolved χ (c), (f). The solid lines (blue) in (a) and (d) are the measured PNSD that can be fitted by a four-mode (a nucleation mode (NM), an Aitken mode (AM), an accumulation mode (AcM) and a coarse mode (CM)) lognormal distribution, which are represented by the thin solid line (orange), the dashed line (green), the dotted line (red), and the dash-dotted line (purple), respectively. The corresponding type and color lines represent the the measured campaign average κ-PDF for each mode in (b) and (e). The dot line in (c) and (f) is the calculated size-resolve ~~κ_{mean}~~κ_{mean}, and the color shaded is the corresponding size-resolved κ-PDF. The solid lines in (c) and (f) is the calculated size-resolved χ.

Table 1. The sketch map of the components and the corresponding indices for the 12 different ~~aerosol populations~~ aerosols in Fig. 2. The LH and MH components are represented by the colors of blue and gray, respectively, V_{LH} and V_{MH} represent their volumes.

Pop.	Sketch map	$V_{\mathrm{LH}} : V_{\mathrm{MH}}$	D_α	D_γ	χ	~~κ_{mean}~~ κ_{mean}
1	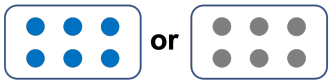	0:6 or 6:0	1	1	0	0.6 or 0.01
2	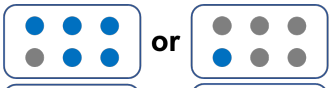	1:5 or 5:1	1	1.569	0	0.502 or 0.108
3	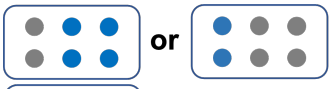	1:2 or 2:1	1	1.890	0	0.403 or 0.207
4	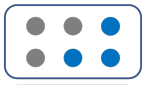	1:1	1	2	0	0.305
5	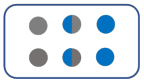	1:1	1.260	2	0.260	0.305
6	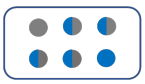	1:1	1.587	2	0.587	0.305
7	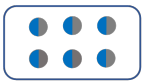	1:1	2	2	1	0.305
8	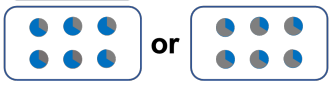	1:2 or 2:1	1.890	1.890	1	0.403 or 0.207
9	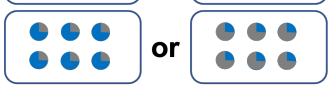	1:3 or 3:1	1.760	1.760	1	0.451 or 0.159
10	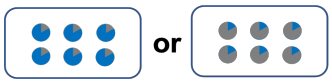	1:6.13 or 6.13:1	1.500	1.500	1	0.517 or 0.093
11	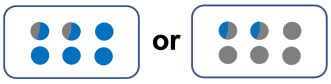	1:6.13 or 6.13:1	1.260	1.500	0.510	0.517 or 0.093
12	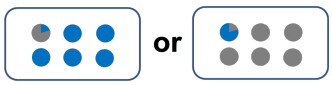	1:6.13 or 6.13:1	1.076	1.500	0.151	0.517 or 0.093

Quantifying particle-to-particle heterogeneity in aerosol hygroscopicity

Liang Yuan[1, 2] and Chunsheng Zhao[2, *]

[1]Chengdu Plain Urban Meteorology and Environment Scientific Observation and Research Station of Sichuan Province, School of Atmospheric Sciences, Chengdu University of Information Technology, Chengdu 610225, China
[2]Department of Atmospheric and Oceanic Sciences, School of Physics, Peking University, Beijing, 100871, China

Correspondence: Chunsheng Zhao (zcs@pku.edu.cn)

Abstract. The particle-to-particle heterogeneity in aerosol hygroscopicity is crucial for understanding aerosol climatic and environmental effects. The hygroscopic parameter κ, widely applied to describe aerosol hygroscopicity for aerosols both in models and observations, is a probability distribution highly related to aerosol heterogeneity due to the complex sources and aging processes. However, the heterogeneity in aerosol hygroscopicity is not adequately represented in observations and model simulations, leading to challenges in accurately estimating aerosol climatic and environmental effects. Here, we propose an algorithm for quantifying the particle-to-particle heterogeneity in aerosol hygroscopicity, based on information-theoretic entropy measures, by using the data that comes only from the in-situ measurement of the hygroscopicity tandem differential mobility analyzer (H-TDMA). Aerosols in this algorithm are assumed to be simple binary systems consisting of the less hygroscopic and more hygroscopic components, which are commonly used in H-TDMA measurement. Three indices, including the average per-particle species diversity D_α, the bulk population species diversity D_γ, and their affine ratio χ, are calculated from the probability distribution of κ to describe aerosol heterogeneity. This algorithm can efficiently characterize the evolution of aerosol heterogeneity with time in the real atmosphere. Our results show that the heterogeneity varies much with aerosol particle size and large discrepancies exist in the width and peak value of particle number size distribution (PNSD) with varied heterogeneity after hygroscopic growth, especially for conditions with high relative humidity. This reveals a vital role of the heterogeneity in ambient PNSD and significant uncertainties in calculating the climate-relevant properties if the population-averaged hygroscopicity is applied by neglecting its heterogeneity. This work points the way toward a better understanding of the role of hygroscopicity in evaluating aerosol climatic and environmental impacts.

1 Introduction

Aerosol hygroscopicity describes the interaction of aerosol particles and water vapor and severely influences aerosol climatic and environmental effects (Wang and Chen, 2019; Swietlicki et al., 2008; Liu et al., 2013; Tie et al., 2017). It is highly related to the particle-to-particle heterogeneity in aerosol hygroscopicity, which is crucial but not adequately considered in observations and models, posing a challenge in accurately estimating aerosol effects on climate and environment.

Köhler theory (Köhler, 1936) is the basis of the studies on aerosol hygroscopicity. Nowadays, the most widely used parameter to describe aerosol hygroscopicity in observations and models is the hygroscopicity parameter, κ, proposed in κ-Köhler theory

(Petters and Kreidenweis, 2007). κ extends and facilitates the application of Köhler theory (Zieger et al., 2013; Bian et al., 2014; Chen et al., 2014; Tao et al., 2014; Brock et al., 2016) and can be expediently observed under both subsaturated (Liu et al., 1978; Kuang et al., 2017) and supersaturated conditions (Petters and Kreidenweis, 2007; Cai et al., 2018). It can also be derived from the observed chemical composition (Liu et al., 2014). Considering that ambient aerosol particles in an aerosol differ dramatically in chemical composition due to the complex sources and aging processes (Li et al., 2021; Zheng et al., 2021; Pang et al., 2022), in terms of aerosol hygroscopicity, the distribution of the nearly hydrophobic (NH), the less hygroscopic (LH), and the more hygroscopic (MH) components (Liu et al., 2011; Tan et al., 2013b; Yuan et al., 2020) vary between and within particles, such particle-to-particle heterogeneity in aerosol hygroscopicity results in a probability distribution of κ (κ-PDF) for an aerosol (Su et al., 2010). Among the three above-mentioned observing techniques, although the hygroscopicity tandem differential mobility analyzer (H-TDMA) can directly achieve κ-PDF under subsaturated condition, which is essential to investigate the hygroscopicity and activation property of aerosols, most studies focus on the analysis and application of the population-averaged κ (κ_{mean}) by neglecting the heterogeneity (Chen et al., 2014; Tao et al., 2014; Brock et al., 2016; Kuang et al., 2017; Liu et al., 1978; Cai et al., 2018; Liu et al., 2014; Yuan et al., 2020; Wang et al., 2018), leading to uncertainties in the estimation of aerosol impacts on climate and environment.

Many research fields face the problem of heterogeneity involving the diversity of variables or issues. The diversity was first quantified in Whittaker (1972) by introducing the information-theoretic entropy in ecology and then in many other fields, including economics (Drucker, 2013), immunology (Tsimring et al., 1996), neuroscience (Strong et al., 1998), and genetics (Falush et al., 2007). Riemer and West (2013) applied it in atmospheric science for the research of aerosol mixing state. By referring to Whittaker (1972) and Riemer and West (2013), the impact of the mixing state of black carbon-containing (BC-containing) particles on light absorption enhancement was investigated, which showed that absorption is strongly affected by the heterogeneity of BC-containing aerosol and explained that the discrepancy between simulated and observed absorption enhancement accounts for the particle-to-particle heterogeneity in composition (Fierce et al., 2016, 2020; Zhao et al., 2021). How crucial the heterogeneity in aerosol hygroscopicity is for the highly climate-relevant aerosol size distribution, optical, and activation properties? However, to the best of the authors' knowledge, most studies are not focused on quantitatively evaluating the heterogeneity concerning aerosol hygroscopicity for in-situ measurements.

Given these considerations, we proposed an algorithm for quantifying the particle-to-particle heterogeneity in aerosol hygroscopicity in the real atmosphere. This algorithm is based on information-theoretic entropy measures, employing observed data from the in-situ measurement of H-TDMA. In the following, section 2 described the algorithm in detail and the interpretation of the results from the algorithm was presented in section 3. The importance of the heterogeneity and the application of the algorithm were discussed and also included in section 3. The last section came the conclusions.

2 Data and Methods

2.1 Measurement site

The campaign was implemented for two periods from 23 January to 25 February and 19 July to 8 September 2019, respectively, at the meteorological station (30.58°N, 103.98°E) inside the campus of Chengdu University of Information and Technology (CUIT) located in Shuangliu district, southwest of the main urban area of Chengdu, China. The elevation of the observation site is approximately 500 m. Fig. S1 in the supplemental file shows the map of the site. It is surrounded by residential neighbourhoods with no nearby sources of significant industrial pollution. Aerosol particles here are representative of the urban environments. More details can be found in Yuan et al. (2020)

2.2 Data of H-TDMA measurement

A custom-built H-TDMA designed by Tan et al. (2013a) was employed to obtain the hygroscopic properties for aerosol particles with dry diameters $D_{\mathrm{p}}(\mathrm{Dry})$ of 40, 80, 110, 150, and 200 nm. The schematic structure of the H-TDMA is shown in Fig. S2 in the supplemental file. This H-TDMA was placed in a temperature-controlled (25 °C) container, with an aerosol inlet equipped with a $\mathrm{PM}_{2.5}$ impactor that extended out of the container from the roof and set approximately 3 m above ground. It mainly consists of two differential mobility analyzers (DMA) (Model 3081A, TSI Inc., USA), a humidification system and a condensation particle counter (CPC) (Model 3787, TSI Inc., USA). Aerosol samples with a flow of 0.6 $\mathrm{L}\cdot\mathrm{min}^{-1}$ are first introduced into a Nafion dryer (Model MD-700-24S-3, Perma Pure Inc., USA) by an external vacuum pump to maintain the RH below 10%. These aerosol particles flow through an advanced aerosol X-ray neutralizer (Model 3088, TSI Inc., USA) to be single-charged and are then screened by the first DMA (DMA-1) with set voltages. Subsequently, the selected quasi-monodisperse dry particles feed into a Nafion humidifier (Model PD-07018T-24MSS, Perma Pure Inc., USA) with RH of 90% ($\pm$0.3%). Finally, the PNSDs of humidified particles out of the humidifier are measured by the second DMA (DMA-2) coupled with the CPC. The details of the H-TDMA refer to Yuan et al. (2020).

The growth factor g of the quasi-monodisperse aerosol particles $g[D_{\mathrm{p}}(\mathrm{Dry})]$ selected by DMA-1 equipped in the H-TDMA can be then calculated by:

$$g[D_{\mathrm{p}}(\mathrm{Dry})] = \frac{D_{\mathrm{p}}(\mathrm{RH})}{D_{\mathrm{p}}(\mathrm{Dry})}, \tag{1}$$

where $D_{\mathrm{p}}(\mathrm{RH})$ represents the particle diameter screened by DMA-2 at a specific relative humidity (RH), e.g., 90% in this study. The measured distribution function of g (g-MDF) is calculated from aerosol particle number size distribution (PNSD) counted by the CPC installed downstream of DMA-2. The $\mathrm{TDMA}_{\mathrm{fit}}$ algorithm (Stolzenburg and McMurry, 2008) is employed to convert the g-MDF to the actual probability distribution function (g-PDF) in the campaign (Gysel et al., 2009). For each measured dry diameter, the g-PDFs are thereafter normalized as:

$$\int_{1}^{\infty} c(g)\mathrm{d}g = 1, \tag{2}$$

where, $c(g)$ represents the normalized g-PDF. For each g, κ can be converted using κ-Köhler theory (Petters and Kreidenweis, 2007):

$$\kappa = (g^3 - 1) \times \Big[\frac{1}{RH} \times \exp\Big(\frac{4\sigma_{s/a} M_{\mathrm{w}}}{RT\rho_{\mathrm{w}} D_{\mathrm{p}}(\mathrm{Dry})g}\Big) - 1\Big], \tag{3}$$

where $\sigma_{\mathrm{s/a}}$ of 0.072 $\mathrm{J \cdot m^{-2}}$ is the surface tension of the solution/air interface, M_{w} of 18.015 $\mathrm{g \cdot mol^{-1}}$ is the molecular weight of water, ρ_{w} of 1.0 $\mathrm{g \cdot cm^{-3}}$ is the density of water, R of 8.315 $\mathrm{J \cdot K^{-1} \cdot mol^{-1}}$ is the universal gas constant, and T of 298.15 K is the temperature in Kelvin. Then, the κ-PDF can be obtained and normalized as:

$$\int_{0}^{\infty} c(\kappa)\mathrm{d}\kappa = 1, \tag{4}$$

where $c(\kappa)$ is the normalized κ-PDF as the examples shown in Fig. 1.

2.3 Calculation of the heterogeneity in aerosol hygroscopicity

The particle-to-particle heterogeneity in aerosol hygroscopicity is calculated by using the H-TDMA measured κ-PDF (e.g. the exmaples in Fig. 1). The key assumption is that an aerosol containing N aerosol particles is a binary system consisting of the LH and MH components with respective κ of 0.01 (κ_{LH}) (typical for organics) and 0.6 (κ_{MH}) (typical for sulphate and nitrate). Each aerosol particle in the population contains one or two of the LH and MH components and thus their κ varied between 0.01 and 0.6. κ-PDF of the aerosol can be considered as the normalized aerosol number fractions varied with κ between 0.01 and 0.6 (Fig. 1). The volume fraction of these two components in each aerosol particle can be calculated based on κ according to the ZSR rule (Zdanovskii, 1948; Stokes and Robinson, 1966).

By refering to information-theoretic entropy measures (Whittaker, 1972; Riemer and West, 2013; Zhao et al., 2021), three indices, including the average per-particle species diversity D_α, the bulk population species diversity D_γ, and their affine ratio χ, are calculated to together describe the heterogeneity. The details are described as follows:

Firstly, for the aerosol with a given dry diameter and a known κ-PDF with X bins, the volume fraction of the LH and MH components at bin i (i=1, 2, 3, …, X), $P_{i,\mathrm{LH}}$ and $P_{i,\mathrm{MH}}$, can be calculated by the combination of

$$P_{i,\mathrm{LH}} + P_{i,\mathrm{MH}} = 1 \tag{5}$$

and

$$P_{i,\mathrm{LH}} \times \kappa_{\mathrm{LH}} + P_{i,\mathrm{MH}} \times \kappa_{\mathrm{MH}} = \kappa_i, \tag{6}$$

where κ_i is the κ at bin i.

Secondly, the mixing entropy for particles at bin i (H_i) can be calculated by

$$H_i = -P_{i,\mathrm{LH}} \times \ln P_{i,\mathrm{LH}} - P_{i,\mathrm{MH}} \times \ln P_{i,\mathrm{MH}}. \tag{7}$$

Then the average particle mixing entropy for the aerosol (H_α) is calculated by

$$H_\alpha = \sum_{j=1}^{N} P_j \times H_j, \tag{8}$$

where, H_j is the mixing entropy for particle j (j=1, 2, 3, ..., N) in the aerosol. P_j is the volume proportion of particle j to the total volume of the aerosol, which is calculated by

$$P_j = \frac{V_j}{V_{\mathrm{total}}} = \frac{1}{N}, \tag{9}$$

because all particles have the same diameters. Considering that particles in the same κ bin have the same physical and chemical properties, they have the same mixing entropy. Eqs. 8 and 9 can be simplified as

$$H_\alpha = \sum_{i=1}^{X} H_i \times c(\kappa)_i \times \Delta\kappa, \tag{10}$$

where, $c(\kappa)_i$ is the probability density value of the normalized κ-PDF at bin i, and $\Delta\kappa$ is the bin width.

Additionally, the population-level mixing entropy (H_γ) is calculated by

$$H_\gamma = -P_{\mathrm{LH}} \times \ln P_{\mathrm{LH}} - P_{\mathrm{MH}} \times \ln P_{\mathrm{MH}}, \tag{11}$$

where, P_{LH} and P_{MH} are the respective volume fraction of the LH and MH components in the population and calculated by

$$P_{\mathrm{LH}} = \sum_{i=1}^{X} P_{i,\mathrm{LH}} \times c(\kappa)_i \times \Delta\kappa \tag{12}$$

and

$$P_{\mathrm{MH}} = \sum_{i=1}^{X} P_{i,\mathrm{MH}} \times c(\kappa)_i \times \Delta\kappa. \tag{13}$$

Thirdly, the per-particle species diversity (D_i), the average per-particle species diversity (D_α) and the population species diversity (D_γ) can be calculated as

$$D_i = e^{H_i}, \tag{14}$$

$$D_\alpha = e^{H_\alpha}, \tag{15}$$

and

$$D_\gamma = e^{H_\gamma}. \tag{16}$$

Finally, a hygroscopic heterogeneity parameter χ can be calculated as

$$\chi = \frac{D_\alpha - 1}{D_\gamma - 1}, \tag{17}$$

which varied from 0% that all particles in the population purely consist of the LH or MH component, to 100% that the LH and MH components are homogeneously distributed across all particles in the population with identical volume fractions.

2.4 Calculation of the size-resolved heterogeneity

A typical four-mode (i. e., a nucleation mode, an Aitken mode, an accumulation mode and a coarse mode) PNSD with a wide size range of 3 nm-10 μm obtained by Ma (2013) is used for the calculation and presentation of the size-resolved heterogeneity. According to the assumption that aerosol particles in a specific mode have common sources or have experienced similar aging processes, the corresponding κ_{mean} and κ-PDF of one mode should be the same. The campaign average κ_{mean} and κ-PDF for particles with diameters of 40 nm, 80 nm, and 200 nm measured by H-TDMA are used to deduce the respective κ_{mean} and κ-PDF for the nucleation mode, Aitken mode, and accumulation mode of the fitted PNSDs. Although the primary chemical compositions in the coarse mode aerosol are nearly hydrophobic, some studies showed that this aerosol is slightly hygroscopic due to the coating in atmospheric aging processes (Hegg et al., 2006; Massling et al., 2009; Liu et al., 2014). However, κ for the coarse mode aerosol is hard to be observed by H-TDMA technique so far, due to the technical bottleneck. Considering that this aerosol has limited influence on radiative forcing and cloud because of its short lifetime and low number concentration, κ for this aerosol is assumed to be 0 as Chen et al. (2012) set. According to the contribution of each mode to the κ_{mean} of specific

particle size, the size-resolved κ_{mean} for aerosol particles ranging from 3 nm-10 μm can be estimated from the known κ_{mean} of each mode ($\kappa_{\mathrm{mean},i}$) as:

$$\kappa_{\mathrm{mean}}(D_{\mathrm{p}}) = \frac{\sum_{i=1}^{4} \kappa_{\mathrm{mean},i} \times N_i(D_{\mathrm{p}})}{\sum_{i=1}^{4} N_i(D_{\mathrm{p}})}. \quad (18)$$

The size-resolved κ-PDF can be calculated using the similar method with Eq. 19:

$$c(\kappa, D_{\mathrm{p}}) = \frac{\sum_{i=1}^{4} N_i(D_{\mathrm{p}}) \times c(\kappa)_i \times \Delta\kappa}{\sum_{i=1}^{4} N_i(D_{\mathrm{p}}) \times \Delta\kappa \times \Delta \log D_{\mathrm{p}}}. \quad (19)$$

Then, the size-resolved heterogeneity $D_\alpha(D_{\mathrm{p}})$, $D_\gamma(D_{\mathrm{p}})$, and $\chi(D_{\mathrm{p}})$ for the wide range of 3 nm -10 μm can be obtained by using Eqs. 5-17.

3 Results

3.1 Diagram for particle-to-particle heterogeneity in aerosol hygroscopicity

From the calculation of Eqs. 15-17, D_α can represent the average of the effective number of species existing in each particle and D_γ can represent the effective number of species in the population. Note that $1 \leq D_\alpha \leq D_\gamma$. D_α = 1 when all particles are pure while D_α = D_γ when all aerosol particles have identical components. The value of D_γ ranges from 1 to 2 according to the volume ratio of the LH and MH components in the population. Specifically, it is 1 when the population purely consists of the LH or MH component while is 2 when the population has the equivalent volume of the LH and MH components. A triangular region is thus presented in Fig. 2, in which χ is represented by contours.

Figs. 2a-2d show an example of the evolution of the heterogeneity in aerosol hygroscopicity. The distributions of the NH and MH components vary between and within populations, causing different heterogeneities for these aerosols. Twelve red dots in Fig. 2e represent aerosols, each consisting of six aerosol particles with varied fractions of the LH and MH components. Their respective sketch maps and heterogeneity indices are summarized in Table 1, and the corresponding κ-PDFs are listed in Fig. S3 in the supplemental file.

For aerosols with particles purely consisting of the LH component or MH component (e.g., populations 1-4 in Fig. 2e and Table 1), D_α equals 1 and χ equals 0, although D_γ varies from 1 to 2 due to the change of the bulk volume ratio of the LH and MH components. Their κ-PDFs show that κ distributes only at 0.01 for the LH component or 0.6 for the MH component due to the pure component in each particle.

For aerosols with equal bulk volume fractions of the LH and MH components (e.g., populations 4-7 and populations 10-12 in Fig. 2e and Table 1), D_γ have constant values of 2 and 1.5, respectively. However, the different distributions of the LH and MH components in each particle of an aerosol contribute to different D_α and χ. Specifically, the heterogeneous distribution (e.g., populations 4-6 and populations 11-12 in Fig. 2e and Table 1) leads to relatively small values of D_α and χ, and the

dispersed κ-PDF. On the contrary, the homogeneous distribution (e.g., populations 7 and 10 in Fig. 2e and Table 1) generates a narrow κ-PDF, and thus relatively high D_α and χ.

For aerosols consisting of particles with identical volume fractions of the LH and MH components (e.g., populations 7-10 in Fig. 2e and Table 1), equal values of D_α and D_γ for each population result in χ of 1, although the bulk ratio of the LH to MH components changes between populations. Accordingly, their κ-PDFs are concentrated at a single value of κ_{mean}.

From the populations, it can be concluded that the particle-to-particle heterogeneity in hygroscopicity resulting from the distribution discrepancy of the LH and MH components within particles can be quantified according to the κ-PDF using the proposed algorithm of this work, which is of importance to the further analysis of the existing κ-PDF and can help the heterogeneity to be considered in the calculation of aerosol climate-relevant properties.

3.2 Evolution of the heterogeneity in the real atmosphere

In this section, we applied the proposed algorithm to the in-situ measurement of H-TDMA that was implemented for two periods in 2019 located in Chengdu, China. In the following, the expression of the κ-PDF is equivalent to the g-PDF due to their one-to-one corresponding relationship. In order to show the variation characteristics and the significance of D_α, D_γ, and χ in the real atmosphere, especially for the condition that the total hygroscopicity of aerosol remained constant, two episodes with tiny change of κ_{mean} during the observation periods are presented. The 110 nm aerosol is chosen as the example to show the typical evolution processes for aerosol heterogeneity, because it has large number concentration and lies in the transition zone between the diameters that show the processes of gas to particle (<100 nm) and aging (>100 nm) in the atmosphere. The variation of the heterogeneity in 110 nm aerosol can better reflect the evolution of aerosol particles in the real atmosphere and may have a great impact on the direct radiative forcing. The first episode appeared from 22:00 (LST) January 23, 2019 to 08:00 (LST) January 24, 2019, and the other one occurred from 00:00 January 27, 2019 to 12:00 January 27, 2019. The variations of D_α, D_γ, χ, and κ_{mean} during these two episodes are shown in Fig. 3. The tiny change of κ_{mean} indicates the slight variation of the bulk fraction of the LH and MH components in the aerosol. The decreasing trends of D_α and χ reveal that the existing aged aerosols with uniformly distributed LH and MH components among particles at night, indicated by the unimodal distributions of κ-PDF and relatively high χ (0.831 for episode 1 at 22:00 and 0.832 for episode 2 at 00:00), were intruded by the fresh emissions during the midnight as reflected by the bimodal and wider distribution of κ-PDF (Yuan et al., 2020). This process led to component discrepancies among particles in populations and thus the decrease of D_α and χ during the midnight.

The statistical PDF of D_α, D_γ, and χ for aerosols with five measured diameters are shown in Fig. 4. The patterns of the distributions for D_α and D_γ move to larger values with increasing diameter, indicating that the effective number of species increases in aerosols with larger diameter due to the longer aging time in the atmosphere. This trend is more obvious in summer campaign. Taking the aerosol of 110 nm for example, D_α varies between 1.386 and 1.850, and D_γ varies between 1.470 and 2.000 during the winter field measurements. The ranges of D_α and D_γ in summer are 1.280-1.928 and 1.371-2.000, respectively, contributing to a wider distribution of χ. This indicates that the fraction of the LH and MH components varied more pronounced due to the more complex aging processes in summer compared to that in winter. χ ranging from 0.6 to 0.9 reveals the large variation of heterogeneity in aerosol hygroscopicity in the real atmosphere.

The details in the variation characteristics of the heterogeneity and the difference among the aerosols of five measured diameters will be further discussed in our future studies. It can be concluded from the discussion above, aerosols with tiny variation of κ_{mean} can have ever-changing heterogeneity in aerosol hygroscopicity in the atmosphere. The algorithm proposed in this work can efficiently characterize this heterogeneity with time and provide detail information about the evolution of aerosols in the air. More importantly, this algorithm offers an unexplored understanding of the H-TDMA measurement.

3.3 Importance of the heterogeneity in aerosol hygroscopicity

The same bulk volume fraction of the LH and MH components indicates the same κ_{mean} for populations (e.g., populations 4-7 and populations 10-12). This reveals the identical diameter for all particles in each population after hygroscopic growth at high RH. Actually, due to the particle-to-particle heterogeneity in one population, different ratios of the LH and MH components in each particle result in different κ (e.g., particles in each of populations 4-7), which can lead to different ambient number size distributions, especially for the condition with high RH. Fig. 5 depicts a sample of the hygroscopic size distribution, where RH is 90%, for three aerosols with the same κ_{mean} of 0.305 but different χ of 0.653, 0.884, and 0.999, respectively. Each of these three populations contains 1000 aerosol particles with dry diameters of 100 nm. Significant discrepancies can be seen in the number size distribution that the width decreases while the peak value increases with increasing χ after hygroscopic growth. Thus, the heterogeneity in aerosol hygroscopicity plays a significant role in the evolution of aerosol ambient number size distributions, which is a key factor for evaluating aerosol radiative forcing.

3.4 Size-resolved heterogeneity in aerosol hygroscopicity

The heterogeneity for only one size can contribute to dramatically different ambient size distributions, especially for the condition under high RH. Thus, it is urgently needed to figure out how the heterogeneity varies with aerosol size in the real atmosphere. This section discussed the characteristic of the size-resolved heterogeneity in aerosol hygroscopicity.

The PNSD within the range of 3 nm-10 μm is commonly observed by commercial instruments, including the scanning mobility particle sizer (SMPS) and the Wide Range Particle Spectrometer (WPS) around the world (Wu and Boor, 2021). However, the widely used H-TDMA technic can only observe the growth factor of aerosols with limited sizes (generally smaller than 350 nm in the dry condition), e.g., 40, 80, 110, 150, and 200 nm in this study. Recently, Shen et al. (2021) extended the H-TDMA measurement of aerosol hygroscopic properties to 600 nm in the urban environment. Although κ for larger particles (> 1 μm) can be derived from the size-resolved chemical composition (Gysel et al., 2007; Liu et al., 2014), the size-resolved κ with high size and time resolution is scarce and is needed to be observed or reversed by more advanced technology and new algorithms. Fortunately, Chen et al. (2012) provided an approach to derive the size-resolved κ for aerosols within the range of 3 nm-10 μm based on the measured PNSDs and H-TDMA determined κ. They used the κ_{mean} for each measured size by neglecting aerosol heterogeneity. Here, the heterogeneity in aerosol hygroscopicity is considered based on the method provided by Chen et al. (2012).

The typical four-mode PNSD mentioned above is used and shown in Fig. 6a and Fig. 6d. The κ_{mean} and the corresponding κ-PDFs for the nucleation mode, Aitken mode, and accumulation mode are represented by those measured at sizes of 40 nm,

80 nm, and 200 nm, respectively, during the winter (Fig. 6b) and summer (Fig. 6e) campaigns. The calculated size-resolved κ_{mean} are shown in Fig. 6c (winter) and Fig. 6f (summer), in which κ-PDF for each size contributed by the heterogeneity in aerosol hygroscopicity is represented by the contour. The variation of both the size-resolved κ_{mean} and the corresponding κ-PDF are influenced by the contribution of each mode to the total number concentration. The corresponding χ for the size range of 3 nm-10 $\mu\mathrm{m}$ can therefore be calculated by using the framework proposed by this work.

As shown in Fig. 6, the consideration of the heterogeneity provides the size-resolved κ-PDF, which can further show the region where the κ is mostly distributed for aerosols of any size and how aerosol particles evolve with size in the population. For example, although the κ_{mean} for aerosols smaller than 40 nm is 0.131 during the winter campaign, the κ-PDF shows most κ locate at a narrow area lower than 0.05. The continuous evolution of the κ-PDF with sizes smaller than 1 $\mu\mathrm{m}$ indicates that on the one hand, a part of the aerosol particles in the population has increasing hygroscopicity during the aging process of growing up, which is the main reason for the increase of κ_{mean}, on the other hand, NH-dominated particles exist across all sizes. This corresponds to the slight decreasing trend of χ accompanied by a wider area of κ ranging from 0.01 to larger than 0.4, which reflects the heterogeneous distribution of the LH and MH components between aerosol particles within a population during the aging progress.

Additionally, the phenomenon that a sharp decrease of χ close to 0.1 for aerosols larger than 1 $\mu\mathrm{m}$ and the κ-PDFs for this size range shows a very narrow band lying at κ of 0 responds to the assumption that the coarse mode particle is mainly composed of the NH component.

Overall, this newly developed aerosol heterogeneity provides more insight into the evolution of aerosols during the aging processes. The hygroscopicity of an aerosol is complicated and diverse due to the particle-to-particle heterogeneity in aerosol hygroscopicity, if only the κ_{mean} is applied without considering aerosol heterogeneity, significant uncertainty will occur.

4 Conclusions

The particle-to-particle heterogeneity in aerosol hygroscopicity is of great importance for better understanding the impact of hygroscopicity on estimating aerosol climatic and environmental effects. Unfortunately, the heterogeneity has not been paid attention to in previous studies, of which only the population-averaged hygroscopicity parameter, κ_{mean}, is considered, mainly because the heterogeneity is difficult to be quantified in both observations and models.

In this work, we proposed an algorithm to quantify the particle-to-particle heterogeneity in aerosol hygroscopicity from the in-situ measurement for the first time. This algorithm is an innovation on the basis of the mature theory in information-theoretic entropy and the widely used assumption that aerosols are binary systems consisting of the commonly defined LH and MH components from H-TDMA measurement.

Three indices, including the average per-particle species diversity D_α, the bulk population species diversity D_γ , and their affine ratio χ, are calculated from the probability distribution of κ to together describe aerosol heterogeneity. They can efficiently characterize and provide more insight into the evolution of aerosol heterogeneity with time in the real atmosphere during the aging processes.

The heterogeneity varies much with aerosol particle size and large discrepancies can be seen in aerosol particle number size distribution (PNSD) that the width decreases while the peak value of the PNSD increases with increasing χ after hygroscopic growth, especially for conditions with high relative humidity, indicating the vital role of the heterogeniety in the evolution of ambient PNSD.

Considering that PNSD is a key factor for the evaluation of aerosol impacts on radiative forcing, significant uncertainties will occur in calculating the climate-relevant properties if κ_{mean} is applied by neglecting its heterogeneity. Thus, the particle-to-particle heterogeneity in aerosol hygroscopicity is urgently needed to be represented in models. The algorithm proposed by this work, which has the intuitive and quantitative interpretation of aerosol heterogeneity, sheds light on the reanalysis of the existing H-TDMA datasets and could have a large impact on how we use and think about these datasets. It can also provide a bridge for using observations to constrain numerical models to deeply investigate how heterogeneity in aerosol hygroscopicity influences aerosol effects on climate and environment.

Data availability. The data is available at https://doi.org/10.5281/zenodo.7320916.

Author contributions. C.Z. designed the research project and reviewed the manuscript. L.Y. interpreted all results and contributed to writing.

Competing interests. The authors declare no competing interests.

Acknowledgements. The authors acknowledge Dr. Yuzhang Che, Prof. Pengguo Zhao, Dr. Jinhui Gao, and Dr. Hui Xiao for fruitful discussions. This work is supported by the National Science Foundation of China (NSFC) (42275070, 42005072, and 42075086) and the Open Project of Key Laboratory for Aerosol-Cloud-Precipitation of China Meteorological Administration, NUIST (KDW1903).

References

Bian, Y., Zhao, C., Ma, N., Chen, J., and Xu, W.: A study of aerosol liquid water content based on hygroscopicity measurements at high relative humidity in the North China Plain, Atmospheric Chemistry and Physics, 14, 6417–6426, https://doi.org/10.5194/acp-14-6417-2014, 2014.

Brock, C. A., Wagner, N. L., Anderson, B. E., Attwood, A. R., Beyersdorf, A., Campuzano-Jost, P., Carlton, A. G., Day, D. A., Diskin, G. S., Gordon, T. D., et al.: Aerosol optical properties in the southeastern United States in summer–Part 1: Hygroscopic growth, Atmospheric Chemistry and Physics, 16, 4987–5007, https://doi.org/10.5194/acp-16-4987-2016, 2016.

Cai, M., Tan, H., Chan, C. K., Qin, Y., Xu, H., Li, F., Schurman, M. I., Liu, L., and Zhao, J.: The size-resolved cloud condensation nuclei (CCN) activity and its prediction based on aerosol hygroscopicity and composition in the Pearl Delta River (PRD) region during wintertime 2014, Atmospheric Chemistry and Physics, 18, 16 419–16 437, https://doi.org/10.5194/acp-18-16419-2018, 2018.

Chen, J., Zhao, C., Ma, N., Liu, P., Göbel, T., Hallbauer, E., Deng, Z., Ran, L., Xu, W., Liang, Z., et al.: A parameterization of low visibilities for hazy days in the North China Plain, Atmospheric Chemistry and Physics, 12, 4935–4950, https://doi.org/10.5194/acp-12-4935-2012, 2012.

Chen, J., Zhao, C., Ma, N., and Yan, P.: Aerosol hygroscopicity parameter derived from the light scattering enhancement factor measurements in the North China Plain, Atmospheric Chemistry and Physics, 14, 8105–8118, https://doi.org/10.5194/acp-14-8105-2014, 2014.

Drucker, J.: Industrial structure and the sources of agglomeration economies: evidence from manufacturing plant production, Growth and Change, 44, 54–91, https://doi.org/10.1111/grow.12002, 2013.

Falush, D., Stephens, M., and Pritchard, J. K.: Inference of population structure using multilocus genotype data: dominant markers and null alleles, Molecular ecology notes, 7, 574–578, https://doi.org/10.1111/j.1471-8286.2007.01758.x, 2007.

Fierce, L., Bond, T. C., Bauer, S. E., Mena, F., and Riemer, N.: Black carbon absorption at the global scale is affected by particle-scale diversity in composition, Nature communications, 7, 1–8, https://doi.org/10.1038/ncomms12361, 2016.

Fierce, L., Onasch, T. B., Cappa, C. D., Mazzoleni, C., China, S., Bhandari, J., Davidovits, P., Fischer, D. A., Helgestad, T., Lambe, A. T., et al.: Radiative absorption enhancements by black carbon controlled by particle-to-particle heterogeneity in composition, Proceedings of the National Academy of Sciences, 117, 5196–5203, https://doi.org/10.1073/pnas.1919723117, 2020.

Gysel, M., Crosier, J., Topping, D., Whitehead, J., Bower, K., Cubison, M., Williams, P., Flynn, M., McFiggans, G., and Coe, H.: Closure study between chemical composition and hygroscopic growth of aerosol particles during TORCH2, Atmospheric Chemistry and Physics, 7, 6131–6144, https://doi.org/10.5194/acp-7-6131-2007, 2007.

Gysel, M., McFiggans, G., and Coe, H.: Inversion of tandem differential mobility analyser (TDMA) measurements, Journal of Aerosol Science, 40, 134–151, https://doi.org/10.1016/j.jaerosci.2008.07.013, 2009.

Hegg, D., Covert, D. S., Crahan, K., Jonsson, H., and Liu, Y.: Measurements of aerosol size-resolved hygroscopicity at sub and supermicron sizes, Geophysical research letters, 33, L21 808, https://doi.org/10.1029/2006GL026747, 2006.

Köhler, H.: The nucleus in and the growth of hygroscopic droplets, Transactions of the Faraday Society, 32, 1152–1161, https://doi.org/10.1039/tf9363201152, 1936.

Kuang, Y., Zhao, C., Tao, J., Bian, Y., Ma, N., and Zhao, G.: A novel method for deriving the aerosol hygroscopicity parameter based only on measurements from a humidified nephelometer system, Atmospheric Chemistry and Physics, 17, 6651–6662, https://doi.org/10.5194/acp-17-6651-2017, 2017.

Li, W., Teng, X., Chen, X., Liu, L., Xu, L., Zhang, J., Wang, Y., Zhang, Y., and Shi, Z.: Organic coating reduces hygroscopic growth of phase-separated aerosol particles, Environmental Science & Technology, 55, 16 339–16 346, https://doi.org/10.1021/acs.est.1c05901, 2021.

Liu, B., Pui, D., Whitby, K., Kittelson, D. B., Kousaka, Y., and McKenzie, R.: The aerosol mobility chromatograph: a new detector for sulfuric acid aerosols, Atmospheric Environment, pp. 99–104, https://doi.org/10.1016/0004-6981(78)90192-0, 1978.

Liu, H., Zhao, C., Nekat, B., Ma, N., Wiedensohler, A., Van Pinxteren, D., Spindler, G., Müller, K., and Herrmann, H.: Aerosol hygroscopicity derived from size-segregated chemical composition and its parameterization in the North China Plain, Atmospheric Chemistry and Physics, 14, 2525–2539, https://doi.org/10.5194/acp-14-2525-2014, 2014.

Liu, P., Zhao, C., Göbel, T., Hallbauer, E., Nowak, A., Ran, L., Xu, W., Deng, Z., Ma, N., Mildenberger, K., et al.: Hygroscopic properties of aerosol particles at high relative humidity and their diurnal variations in the North China Plain, Atmospheric Chemistry and Physics, 11, 3479–3494, https://doi.org/10.5194/acp-11-3479-2011, 2011.

Liu, X. G., Li, J., Qu, Y., Han, T., Hou, L., Gu, J., Chen, C., Yang, Y., Liu, X., Yang, T., Zhang, Y., Tian, H., and Hu, M.: Formation and evolution mechanism of regional haze: a case study in the megacity Beijing, China, Atmospheric Chemistry and Physics, 13, 4501–4514, https://doi.org/10.5194/acp-13-4501-2013, 2013.

Ma, N.: Aerosol optical and activation properties in the North China Plain, Peking University, 2013.

Massling, A., Stock, M., Wehner, B., Wu, Z., Hu, M., Brüggemann, E., Gnauk, T., Herrmann, H., and Wiedensohler, A.: Size segregated water uptake of the urban submicrometer aerosol in Beijing, Atmospheric Environment, 43, 1578–1589, https://doi.org/10.1016/j.atmosenv.2008.06.003, 2009.

Pang, Y., Wang, Y., Wang, Z., Zhang, Y., Liu, L., Kong, S., Liu, F., Shi, Z., and Li, W.: Quantifying the fractal dimension and morphology of individual atmospheric soot aggregates, Journal of Geophysical Research: Atmospheres, 127, e2021JD036 055, https://doi.org/10.1029/2021JD036055, 2022.

Petters, M. and Kreidenweis, S.: A single parameter representation of hygroscopic growth and cloud condensation nucleus activity, Atmospheric Chemistry and Physics, 7, 1961–1971, https://doi.org/10.5194/acp-7-1961-2007, 2007.

Riemer, N. and West, M.: Quantifying aerosol mixing state with entropy and diversity measures, Atmospheric Chemistry and Physics, 13, 11 423–11 439, https://doi.org/10.5194/acp-13-11423-2013, 2013.

Shen, C., Zhao, G., Zhao, W., Tian, P., and Zhao, C.: Measurement report: aerosol hygroscopic properties extended to 600 nm in the urban environment, Atmospheric Chemistry and Physics, 21, 1375–1388, https://doi.org/10.5194/acp-21-1375-2021, 2021.

Stokes, R. and Robinson, R.: Interactions in aqueous nonelectrolyte solutions. I. Solute-solvent equilibria, The Journal of Physical Chemistry, 70, 2126–2131, https://doi.org/10.1021/j100879a010, 1966.

Stolzenburg, M. R. and McMurry, P. H.: Equations governing single and tandem DMA configurations and a new lognormal approximation to the transfer function, Aerosol Science and Technology, 42, 421–432, https://doi.org/10.1080/02786820802157823, 2008.

Strong, S. P., Koberle, R., Van Steveninck, R. R. D. R., and Bialek, W.: Entropy and information in neural spike trains, Physical review letters, 80, 197, https://doi.org/10.1103/PhysRevLett.80.197, 1998.

Su, H., Rose, D., Cheng, Y., Gunthe, S., Massling, A., Stock, M., Wiedensohler, A., Andreae, M., and Pöschl, U.: Hygroscopicity distribution concept for measurement data analysis and modeling of aerosol particle mixing state with regard to hygroscopic growth and CCN activation, Atmospheric Chemistry and Physics, 10, 7489–7503, https://doi.org/10.5194/acp-10-7489-2010, 2010.

Swietlicki, E., Hansson, H.-C., Hämeri, K., Svenningsson, B., Massling, A., McFiggans, G., McMurry, P., Petäjä, T., Tunved, P., Gysel, M., et al.: Hygroscopic properties of submicrometer atmospheric aerosol particles measured with H-TDMA instruments in various en-

vironments—a review, Tellus B: Chemical and Physical Meteorology, 60, 432–469, https://doi.org/10.1111/j.1600-0889.2008.00350.x, 2008.

Tan, H., Xu, H., Wan, Q., Li, F., Deng, X., Chan, P., Xia, D., and Yin, Y.: Design and application of an unattended multifunctional H-TDMA system, Journal of Atmospheric and Oceanic Technology, 30, 1136–1148, https://doi.org/10.1175/JTECH-D-12-00129.1, 2013a.

Tan, H., Yin, Y., Gu, X., Li, F., Chan, P., Xu, H., Deng, X., and Wan, Q.: An observational study of the hygroscopic properties of aerosols over the Pearl River Delta region, Atmospheric Environment, 77, 817–826, https://doi.org/10.1016/j.atmosenv.2013.05.049, 2013b.

Tao, J., Zhao, C., Ma, N., and Liu, P.: The impact of aerosol hygroscopic growth on the single-scattering albedo and its application on the NO_2 photolysis rate coefficient, Atmospheric Chemistry and Physics, 14, 12 055–12 067, https://doi.org/10.5194/acp-14-12055-2014, 2014.

Tie, X., Huang, R.-J., Cao, J., Zhang, Q., Cheng, Y., Su, H., Chang, D., Pöschl, U., Hoffmann, T., Dusek, U., et al.: Severe pollution in China amplified by atmospheric moisture, Scientific Reports, 7, 1–8, https://doi.org/10.1038/s41598-017-15909-1, 2017.

Tsimring, L. S., Levine, H., and Kessler, D. A.: RNA virus evolution via a fitness-space model, Physical review letters, 76, 4440, https://doi.org/10.1103/PhysRevLett.76.4440, 1996.

Wang, Y. and Chen, Y.: Significant climate impact of highly hygroscopic atmospheric aerosols in Delhi, India, Geophysical Research Letters, 46, 5535–5545, https://doi.org/10.1029/2019GL082339, 2019.

Wang, Y., Li, Z., Zhang, Y., Du, W., Zhang, F., Tan, H., Xu, H., Fan, T., Jin, X., Fan, X., et al.: Characterization of aerosol hygroscopicity, mixing state, and CCN activity at a suburban site in the central North China Plain, Atmospheric Chemistry and Physics, 18, 11 739–11 752, https://doi.org/10.5194/acp-18-11739-2018, 2018.

Whittaker, R. H.: Evolution and measurement of species diversity, Taxon, 21, 213–251, https://doi.org/10.2307/1218190, 1972.

Wu, T. and Boor, B. E.: Urban aerosol size distributions: a global perspective, Atmospheric Chemistry and Physics, 21, 8883–8914, https://doi.org/10.5194/acp-21-8883-2021, 2021.

Yuan, L., Zhang, X., Feng, M., Liu, X., Che, Y., Xu, H., Schaefer, K., Wang, S., and Zhou, Y.: Size-resolved hygroscopic behaviour and mixing state of submicron aerosols in a megacity of the Sichuan Basin during pollution and fireworks episodes, Atmospheric Environment, 226, 117 393, https://doi.org/10.1016/j.atmosenv.2020.117393, 2020.

Zdanovskii, A.: New methods for calculating solubilities of electrolytes in multicomponent systems, Zh. Fiz. Khim, 22, 1478–1485, 1948.

Zhao, G., Tan, T., Zhu, Y., Hu, M., and Zhao, C.: Method to quantify black carbon aerosol light absorption enhancement with a mixing state index, Atmospheric Chemistry and Physics, 21, 18 055–18 063, https://doi.org/10.5194/acp-21-18055-2021, 2021.

Zheng, Z., West, M., Zhao, L., Ma, P.-L., Liu, X., and Riemer, N.: Quantifying the structural uncertainty of the aerosol mixing state representation in a modal model, Atmospheric Chemistry and Physics, 21, 17 727–17 741, https://doi.org/10.5194/acp-21-17727-2021, 2021.

Zieger, P., Fierz-Schmidhauser, R., Weingartner, E., and Baltensperger, U.: Effects of relative humidity on aerosol light scattering: results from different European sites, Atmospheric Chemistry and Physics, 13, 10 609–10 631, https://doi.org/10.5194/acp-13-10609-2013, 2013.

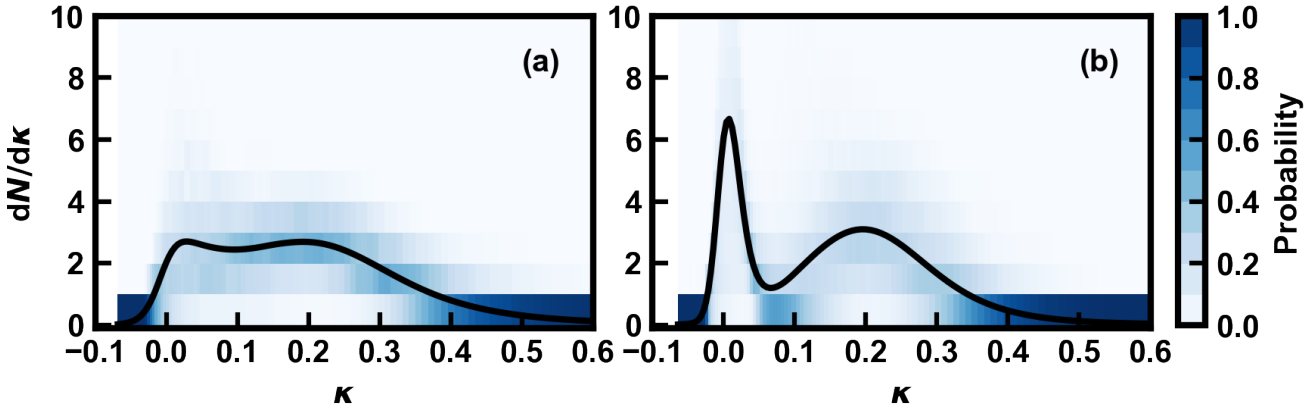

Figure 1. Typical κ-PDF for 100 nm aerosols in winter (a) and summer (b) measured by H-TDMA over Chengdu. The shaded is the frequency distribution of κ-PDF, and the solid lines show the campaign average of κ-PDF.

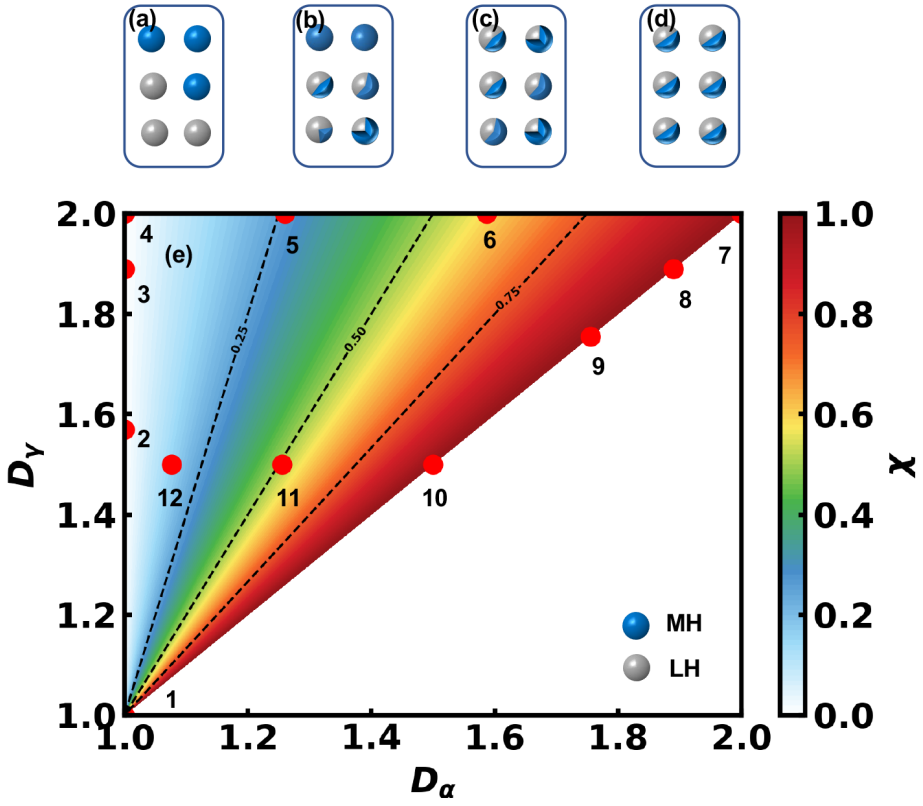

Figure 2. Example of the evolution of the heterogeneity in aerosol hygroscopicity (a-d) and diagram for the relationship among D_α, D_γ, and χ (e). Twelve different aerosols, each of which consists of six particles as shown in Table 1, are represented by the red points.

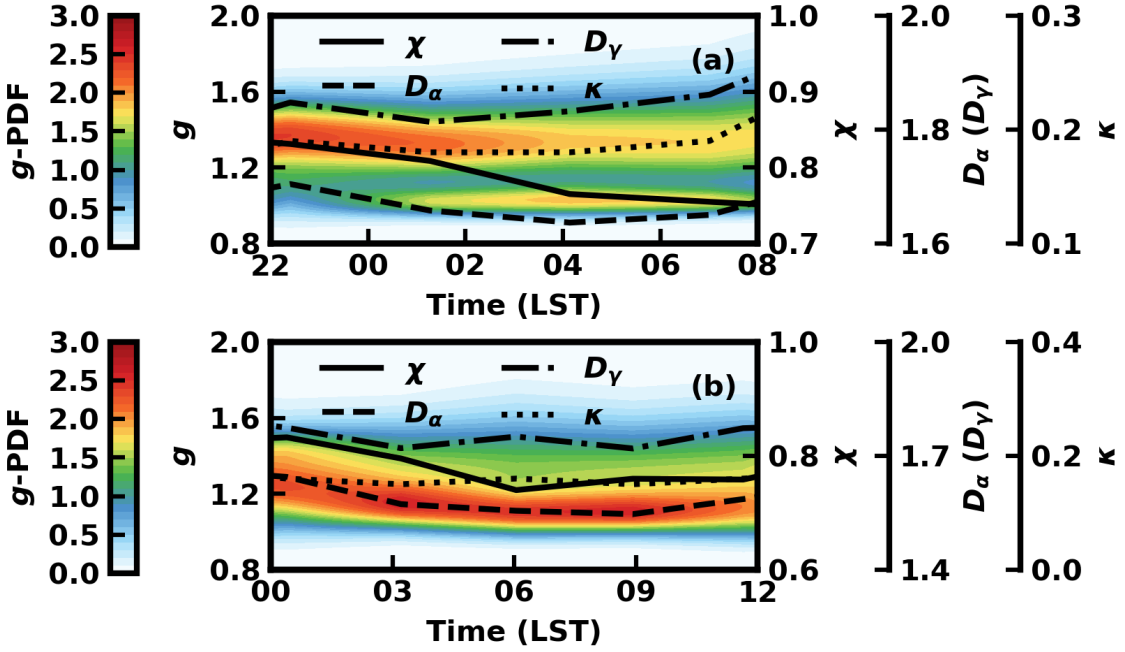

Figure 3. The variation of κ-PDF, D_α, D_γ, and χ during two typical evolution processes for 110 nm aerosols with tiny changes of κ_{mean} on January 23, 2019 (a) and January 27, 2019 (b).

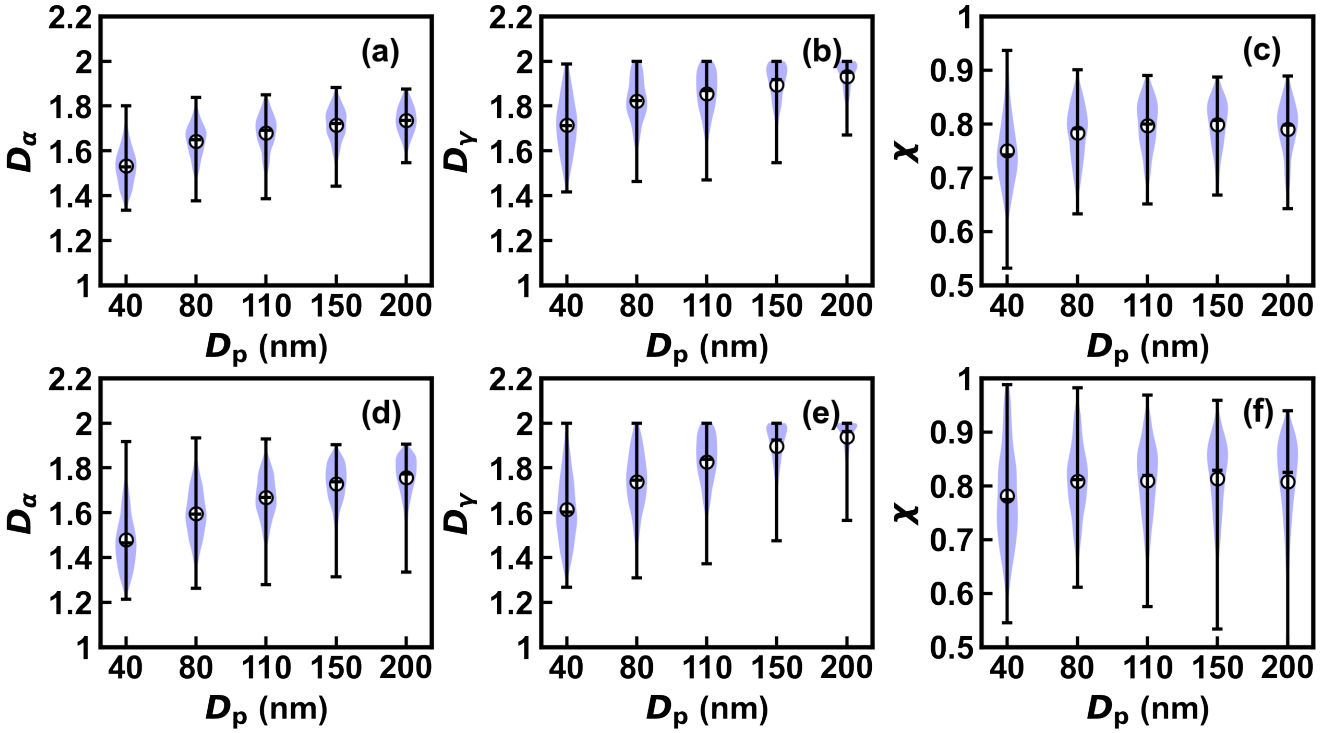

Figure 4. The statistical of D_α, D_γ, and χ for aerosols of five measured diameters in winter (a), (b), (c) and summer (d), (e), (f). The shaded is the frequency distribution of the indices. The three bars on whisker for each diameter from the bottom to the top are the minimum, median, and maxmum, and the circles represent the average of the indices.

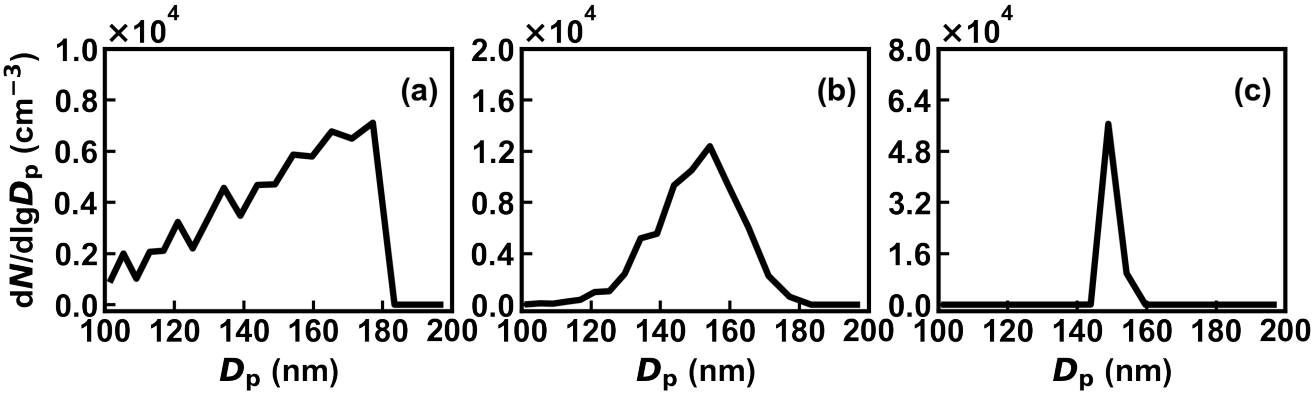

Figure 5. Aerosol particle size distributions after hygroscopic growth at RH of 90% for three aerosols with χ of 0.653 (a), 0.884 (b), and 1 (c), respectively. Each of these three populations has the same κ_{mean} of 0.305 and contains 1000 aerosol particles with dry diameters of 100 nm.

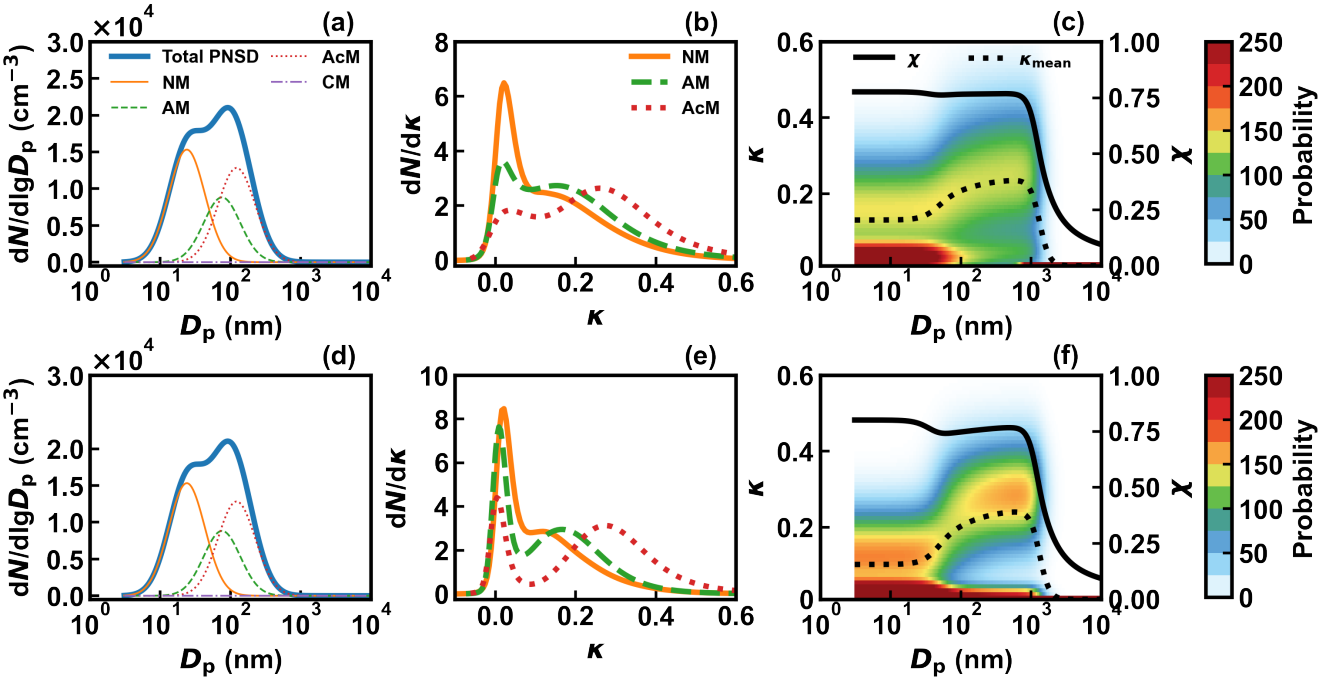

Figure 6. The typical PNSD (a), (d) and the κ-PDF during the winter (b) and summer campaigns (e) used for calculating the size-resolve κ_{mean}, the size-resolved κ-PDF, and the corresponding size-resolved χ (c), (f). The solid lines (blue) in (a) and (d) are the measured PNSD that can be fitted by a four-mode (a nucleation mode (NM), an Aitken mode (AM), an accumulation mode (AcM) and a coarse mode (CM)) lognormal distribution, which are represented by the thin solid line (orange), the dashed line (green), the dotted line (red), and the dash-dotted line (purple), respectively. The corresponding type and color lines represent the the measured campaign average κ-PDF for each mode in (b) and (e). The dot line in (c) and (f) is the calculated size-resolve κ_{mean}, and the color shaded is the corresponding size-resolved κ-PDF. The solid lines in (c) and (f) is the calculated size-resolved χ.

Table 1. The sketch map of the components and the corresponding indices for the 12 different aerosols in Fig. 2. The LH and MH components are represented by the colors of blue and gray, respectively, V_{LH} and V_{MH} represent their volumes.

Pop.	Sketch map	$V_{\mathrm{LH}} : V_{\mathrm{MH}}$	D_α	D_γ	χ	κ_{mean}
1	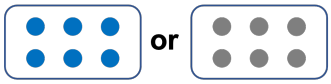	0:6 or 6:0	1	1	0	0.6 or 0.01
2	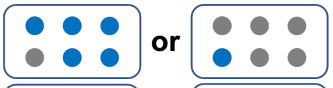	1:5 or 5:1	1	1.569	0	0.502 or 0.108
3	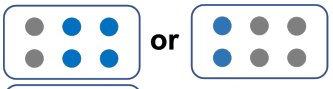	1:2 or 2:1	1	1.890	0	0.403 or 0.207
4	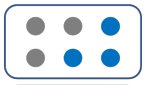	1:1	1	2	0	0.305
5	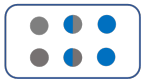	1:1	1.260	2	0.260	0.305
6	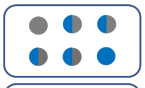	1:1	1.587	2	0.587	0.305
7	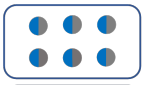	1:1	2	2	1	0.305
8	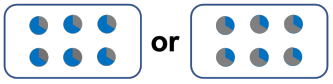	1:2 or 2:1	1.890	1.890	1	0.403 or 0.207
9	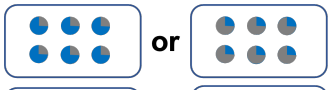	1:3 or 3:1	1.760	1.760	1	0.451 or 0.159
10	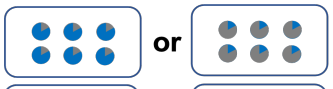	1:6.13 or 6.13:1	1.500	1.500	1	0.517 or 0.093
11	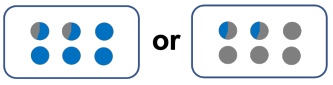	1:6.13 or 6.13:1	1.260	1.500	0.510	0.517 or 0.093
12	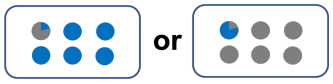	1:6.13 or 6.13:1	1.076	1.500	0.151	0.517 or 0.093